Determining stoichiometric parameters in macrophyte beds with a fixed biomass respirometer

Susana Perdigão Ho

Dissertação para obtenção do Grau de Mestre em

Engenharia do Ambiente

Orientadora: Prof.ª Ana Fonseca Galvão

Co-orientadora: Eng.ª Joana Martins Pisoeiro

Júri

Presidente: Prof. Tiago Morais Delgado Domingos

Orientadora: Prof.ª Ana Fonseca Galvão

Vogal: Prof.ª Helena Maria Rodrigues Vasconcelos Pinheiro

Novembro de 2018

Acknowledgements

Gostaria de expressar a minha sincera gratidão à minha orientadora, Prof. Ana Galvão, que me fez sentir bem-vinda desde o primeiro dia, pelo seu incansável apoio académico e moral, pela sua paciência e entusiasmo. Deixo uma sentida palavra de agradecimento à minha co-orientadora, Engª. Joana Pisoeiro em quem encontrei uma ética de trabalho exemplar, pelo seu vital apoio, pela sua companhia para tantos cafés, almoços tardios e pela sua amizade.
Aos meus colegas de laboratório e amigos, Filipa e Filipe, pela sua disponibilidade e companhia.
À minha grande companheira deste semestre, serei para sempre grata à Catarina por todo o seu apoio e amor.

À minha querida Avó Bi, que é o meu porto de abrigo, a minha cúmplice, o meu exemplo de Mulher e a melhor parte de mim. Embora tenha tentado várias vezes, nunca serei capaz de pôr por escrito o quanto a Avó é fundamental.
À minha Mãe que me deu pernas para andar e infinitas palavras e gestos de carinho que guardo no coração e levo comigo para onde vou. Ao meu Pai por me ter ensinado a garra e o trabalho, mas também a honestidade e a modéstia. À minha querida Ritinha por sentir sempre telepaticamente quando preciso da sua companhia e de um abraço apertadinho. À minha Vovó Kina, agradeço todos os dias que me telefona com preocupação e sempre que me senta à mesa como se fosse a minha última refeição. Aos meus primos Afonso, Gracinha, Ga, Teresinha e Zé, que na realidade são meus irmãos, pelo seu inestimável companheirismo e amor incondicional. À minha melhor amiga Marta, que ilumina uma sala quando se ri e com quem tenho as melhores conversas sem dizer uma palavra. À Bea e à Rita pela sua amizade ao longo deste percurso.
A si, Avô Ho Ka Kui, a quem não posso agradecer em pessoa por tudo o que me ensinou. Penso em si todos os dias e assino tudo com a sua caneta.

Abstract

Treatment wetlands (TW) are a low-cost and environmental technology for wastewater treatment and their increasing interest has motivated substantial development in the models used to describe Nature-based processes to treat wastewater. However, the inevitable unpredictability of biological processes makes the modelling task challenging.

Models for activated sludge (AS) have been successfully developed over the years, constituting a solid base for TW modelling. However, several authors have been presenting different insights and terminologies, and to this date a universal model capable of explaining the wide range of biological processes that take place in a TW is yet to be presented.

In an attempt to contribute to the current state of the art, the present work was developed with the purpose of assessing stoichiometric parameters of heterotrophic growth and storage yields of a lab-scale horizontal sub-surface flow (HSSF)TW with a fixed liquid phase – stationary gas flowing liquid (LSF) respirometer. This study focused on the characterization of a lab-scale TW (two types of medium beds with COD feeding concentrations of 800 and 1600 mgO_2/L), the construction and characterization of the respirometer, the respirometric tests with an acetate solution and their translation into oxygen uptake rate (OUR) curves for the calculation of heterotrophic growth yield, Y_H and storage yield, Y_{HSTO}, both in mg_{COD}/mg_{COD}.

It was found that the tested methodology was capable of presenting yield values for 18 respirometry tests and that those values were fairly in accordance with the literature, with average Y_H and Y_{HSTO} of 0,66 and 0,75 for beds fed with a COD of 1600 mgO_2/L and 0,67 and 0,83 for beds fed with a COD of 800 mgO_2/L.

Keywords: Horizontal sub-surface flow constructed wetlands; respirometry; stoichiometric parameters; biological modelling; sustainability.

Table of contents

List of Figures

List of Tables

1. Introduction

1.1 Motivation

Clean water is of the utter most importance to assure a proper quality of life. The increasing demographic trends and the fast pace of technological, industrial and agricultural development put tremendous pressure in responding to the amount of wastewater produced around the world every day.

As of 2016, it is reported that water pollution is seeing an increase since the 1990's in Latin America, Africa and Asia, mainly due to the growth in wastewater loadings to rivers and lakes. The most vulnerable populations to the consequences of water quality are women who are responsible for household chores which mainly involve the use of water, children who collect the water and often play near contaminated water sites, low income fishers and the low-income rural population that consumes the contaminated fish (UNEP 2016).

It is therefore necessary to enhance known and used models for wastewater treatment, as well as to come up with new ways of meeting this high demand. In this sense, the present thesis was developed with the aim of supplying experimental data to solidify the models so far designed for constructed wetlands – treatment wetlands (TW). This emerging technology bases itself on Nature and has shown its potential through effective results, low costs and low environmental impact. It is also of particular interest for application in developing countries' rural areas, where natural systems are preferred for economic and cultural reasons, opposed to traditional wastewater treatment plants.

1.2 Objectives

The purpose of this thesis is the use of respirometry for determination of stoichiometric parameters for microbial metabolism modelling, in a lab-scale functioning horizontal sub-surface flow (HSSF) treatment wetland. Particularly, the aim of this work is the determination of values for heterotrophic growth and storage yield coefficients, Y_H and Y_{HSTO}, with the intent of pursuing the findings of Pisoeiro et al. (2017) in this field.

Given that respirometric techniques have so far mainly been used in activated sludge studies, several possibilities are still available for the application of this tool in treatment wetlands. For this reason, another of the objectives of the present work is to assess the viability of a liquid phase – stationary gas and flowing liquid respirometer, LSF, applied in the context of treatment wetland study.

Recent developments in modelling processes in treatment wetlands, such as the Constructed Wetland Model 1 (CWM1) also motivated the objective of supplying further experimental data for their consolidation.

1.3 Thesis structure

Five chapters make up this thesis, where 1, 2 and 3 provide a state-of-the-art starting point for chapters 4 and 5, where the procedures, results and discussion of the present work are described.

After the introduction to the subject in Chapter 1, the main definitions, characteristics and processes that take place in treatment wetlands are described, followed by the evolution of models from

activated sludge to treatment wetlands. The last subsection in Chapter 2 provides the theoretical basis of respirometry as a tool for assessment of microbial and stoichiometric parameters, as well as some of the work that has been developed in this sense.

Chapter 3 is destined to describe the treatment wetland used, the assembly and characteristics of the LSF respirometer, and the respirometric procedures.

The results obtained from the respirometric techniques and their confrontation with the work by Pisoeiro et al. (2017) are gathered in Chapter 4, and finally Chapter 5 presents the main conclusions taken from this work, as well as future works suggestions.

2. Literature review

2.1 General description of wetland

Constructed wetlands have become a very interesting tool for wastewater treatment for a number of reasons, such as their low-cost, low-maintenance and low-environmental impact characteristics, which, depending on the case, offer a complementary solution or an alternative for traditional wastewater treatment plants, based on activated sludge models.

Their principle is based on the wetland ecosystem, in which water inundates land, permanently or seasonally, saturating the soil. The wetland is a combination of several actors, such as water, substrate (granular material), plants, microorganisms, litter and invertebrates. In conjunction, these allow for physical, chemical and biological processes which treat and clean contaminated water. The inlet wastewater flows over or through the substrate and is discharged at the outlet, where it is clean from contaminants.

A basin is excavated and filled with the substrate (gravel, sand, rock or soil) and the water level is maintained either above or just below the surface of the substrate. In cases where groundwater contamination is of concern, a liner is placed under the substrate. The top of the substrate is planted, where the root system of these plants develops (Shrestha, 2008).

In the context of water treatment, there may be some disagreement in the use of the term “wetland”. In Nature, this system is composed by water, plants and a media. When it doesn’t hold any plants, it may be defined as a pond, soil or a gravel filter. Given this fact, and in an attempt to unify the terminology, most authors – as well as this thesis – use the term “treatment wetland” to refer to these engineered structures.

2.1.1 Horizontal and Vertical flow treatment wetlands

There are several classifications of treatment wetlands, which categorize them according to their type of plants, type of wastewater, treatment level of wastewater and type of substrate, to name a few. The flow pattern in the wetland system has been the classification predominantly used in the research and implementation of the present thesis. The referred classification starts with the distinction between free water surface flow (FWSF) and subsurface flow (SSF): in the case of FWS, the water level is kept above the planted substrate, requiring thus plants that are able to survive to permanently flooded conditions. In this type of TW, the water flow is always horizontal. Regarding SSF TW, the water flows below the surface of the porous media that makes up the substrate (Dotro et al., 2018). Furthermore, SSF treatment wetlands are grouped either as vertical flow (VF) or horizontal flow (HF), the latter being the type of treatment wetland here approached.

Vertical flow treatment wetlands have their wastewater fed from the top and percolated through the bed, where its collection is carried out by a drainage network at the base.

Horizontal flow treatment wetlands carry the waste water horizontally under the surface of the substrate, until it reaches the outlet.

The main difference between the two types of treatment wetlands is the manner in which the wastewater is fed: in VFTW, the sewage water is pumped from the top in defined intervals of for example 2 to 6
hours, depending on the design and treatment level desired. In HFTW, the wastewater fills the spaces between the substrate, according to the volume of wastewater received at each time. The main advantage of a VFTW however is that it takes up 2/3 of the space necessary to install an HFTW (Montgomery, n.d.).

Another significant difference in the treatment efficiency of HF and VF is the ability to remove nutrients. Unlike HFTW, the VFTW possess the ability of nitrification - removal of nitrogenous compounds from the water, via the microbe-mediated process of oxidizing ammonia (Bioscience 2016). This mechanism is allowed by the oxygen transfer that takes place in a VFTW, as a result of its characteristic intermittent wastewater dosing system: after the first large batch of sewage water has percolated through the system, the spaces between the substrate are refilled with air. The load of waste water fed next will trap this air which, in conjunction with the aeration resultant by the rapid loading of sewage water, will lead to a good oxygen transfer allowing thus for nitrification. However, if the substrate media is not correctly selected, VFTW can potentially become clogged.

On the other hand, HFTW are of great interest when it comes to organic pollutants removal: COD, BOD and TSS. Once the wastewater is fed horizontally at sub-surface level, its passage will allow for contact with three distinct areas: aerobic, anoxic and anaerobic. The aerobic zones are located around the rhizosphere and the water is treated through microbiological degradation, physical and chemical processes.

2.2 Wastewater composition – domestic sewage

Domestic sewage is composed by blackwater (resultant from excreta, urine and fecal sludge) and greywater (originated from water use in the kitchen and bathroom).
The composition of wastewater from domestic origin is divided into 99,9% of water and 0,1% of pollutants. That small fraction that represents the concern for wastewater treatment is made up by organic and inorganic matter, suspended and dissolved solids and microorganisms. The parameters that allow for the assessment of the quality of the wastewater are physical, chemical and biological.

The main physical characteristics of domestic wastewater are temperature, turbidity, color and odor. The chemical characteristics are composed by total solids, organic matter, nutrients such as nitrogen and phosphorus, pH, alkalinity, chlorides, oils and grease.
The biological fraction of wastewater includes organisms such as bacteria, viruses, protozoa, algae, archae, fungi and helminths.

In the context of wastewater treatment, the parameters worth highlighting are the total solids, the organic matter (via its indicators), nitrogen, phosphorus and contamination with faecal microorganisms (via its indicators) (Sperling 2008).

2.2.1 Solids

Domestic sewage solids are classified according to their size, chemical characteristics and settleability.

The size classification of solids divides them into three categories which, from smaller to bigger are given by dissolved, colloidal and suspended. When using a filter paper, for example, if the solids are able to pass through it, they are dissolved (pore diameter from 10^{-6} to 10^{-3} μm); if they are retained, then the solids are suspended (pore diameter from 0.2 to 0.45 μm). The intermediate range is occupied by colloidal solids, with diameters varying from 10^{-3} to 1 μm.

In case organic matter or nutrients are associated to solids, if their size is correspondent to dissolved solids, these are referred to as soluble (soluble BOD, for example); if these compounds are associated to suspended solids, the term used for them is particulate (particulate phosphorus, for example).

The solids are classified by their chemical character – fixed or volatile solids – according to their combustible or non-combustible nature, which is assessed by the combustion at 550º C: what is left behind corresponds to the inert fraction, the inorganic matter. This inorganic fraction makes up the fixed solids. The organic fraction is designated by volatile solids.

Furthermore, solids are considered settleable if they behave like so in a resting period of 1 hour and its volume is expressed in terms of mL/L of solution (Sperling 2008).

2.2.2 Organic matter

Organic matter (OM) originates from dead organisms (plants and animals), organic excretions and non-biogenic carbon composts (Sousa 2001). It is composed by biopolymers like proteins, carbohydrates and lipids easily degraded by microorganisms, and by recalcitrant materials – resistant to decomposition – such as lignin and hemicellulose (Vymazal et al., 2009).

When an excess of easily biodegradable matter enters surface waters, organic pollution takes place. When this matter is decomposed by bacteria and other microorganisms, the resulting oxygen consumption may reach the level of depletion, negatively affecting the aquatic fauna (UNEP 2016). The consumption of OM by the microorganisms either in the wastewater or in the receiving water body can be used for two purposes: to obtain energy – catabolism – or to incorporate such matter in the cellular material – anabolism.

This class of compounds can be divided according to its form and size and in terms of its biodegradability. On the other hand, it can be measured in terms of its indicators, which give the information of the amount of organic matter through the measurement of oxygen consumption (indirect methods), or measurement of organic carbon (direct methods).

The classification of OM according to its form and size divides it in two classes designated as suspended and dissolved. In terms of biodegradability, organic matter is either inert or biodegradable (Sperling 2008).

In order to quantify the OM and given that it is nearly impossible to individually determine each organic compound, certain indicators are used under the premise of what is common to each organic

compound, which is the fact that they are oxidizable and that they all have organic carbon in their composition.

The two tests used with the oxidation principle are the biochemical oxygen demand (BOD) test, and the chemical oxygen demand (COD) test. To determine the organic carbon, the total organic carbon (TOC) test is used.

Biochemical oxygen demand measures the oxygen consumed during organic matter oxidation carried out by microorganisms (biomass) in aerobic conditions. This measurement is made in terms of milligrams of oxygen per liter of solution (water). When biomass degrades the organic matter in wastewater, the level of dissolved oxygen decreases. For this reason, the oxygen consumed in the process is proportional to the amount of decomposable organic matter. Typically, natural clean waters have a BOD of 5 mgO_2/L or less, whereas sewage water BOD ranges from 150 to 300 mgO_2/L (Alam 2015) or 100 to 400 mgO_2/L, depending on the authors (Golconda 2016).

Chemical oxygen demand represents the amount of oxygen required to chemically oxidize organic matter to CO_2. Again, COD is represented by milligrams of oxygen consumed by liter of solution (mg/L). The organic matter is oxidized by a strong oxidizing agent, like potassium dichromate ($K_2Cr_2O_7$). Like BOD, the more polluted the water is, the higher the COD (Alam 2015).

Given that the complete oxidation of all organic matter by microorganisms depends on the size and the nature of the molecules (the smaller ones are readily available but bigger molecules, colloidal and suspended matter must first be hydrolyzed), BOD tests take a long time – around 20 or more days for domestic sewage (Golconda 2016). This measurement results in the ultimate BOD. In order to produce faster and standardized tests, BOD_5 tests are carried out instead, measuring the oxygen consumption in 5 days at 20º C (temperature influences the metabolism of bacteria).

On the other hand, COD tests take up to 2 hours but do not differentiate between biological oxidizable and non-oxidizable matter. Given that is not possible to distinguish between the two, the COD/BOD_5 ratio was introduced. It was found that this ratio does not vary significantly for a particular waste, and for this reason, it is a reliable measurement of the biodegradable fraction. The higher the ratio, the lower the biodegradable fraction is and the higher the inert fraction is ($COD/BOD_5 > 3.5$), and vice-versa ($COD/BOD_5 < 2.5$). Typical values for raw domestic sewage COD/BOD_5 ratio range between 1.7 and 2.4.

The ratio between BOD ultimate and BOD_5 is also worthy of note. In typical domestic sewage, BOD_u/BOD_5 is 1,46 mg BOD_u/mg BOD_5. Given that the reciprocal is still true, then 1/1,46 = 0,68 mgBOD 5/mg BOD_u. This means that by the fifth day of the BOD test, 68% of the organic matter has been oxidized and 68% of the total oxygen consumption was reached by the fifth day.

Three conditions regarding the ratios above described are also relevant: the first one is that they can never be less than 1; secondly, the ratios increase from untreated to biologically treated water; and lastly, the higher the efficiency of the treatment is, the higher the ratios are (Sperling 2008).

In Portugal, the limits that must be complied before returning the treated water to a natural water body are the following: BOD_5 without nitrification = 25 mgO_2/L, COD = 125 mgO_2/L (Ministério do Ambiente 1997).

2.2.3 Nitrogen, N

The presence of nitrogen compounds in abnormal quantities is of great concern for different reasons. It causes eutrophication of the water bodies. On the other hand, nitrogen pollution may deplete dissolved oxygen as a result of its reactions. In its free form, nitrogen is toxic to certain organisms such as fish, and finally, it is associated to diseases such as methaemoglobinaemia. The latter makes oxygen unable to be transported by the blood stream, resulting in a series of complications which can ultimately lead to death.

Nitrogen can be found under two forms: organic and inorganic. Organic nitrogen appears through proteins, amino acids, urea, amino sugars and humic substances, whereas inorganic nitrogen takes form as total ammonia nitrogen (NH_3 + NH_4^+), nitrates (NO_3) and nitrites (NO_2^-).
The sum of the above-mentioned organic nitrogen, total ammonia, nitrite and nitrate results in total nitrogen. Total Kjeldahl nitrogen (TKN) is used to express the sum of organic N and total ammonia nitrogen. TKN is the predominant form of nitrogen in raw domestic sewage (Sperling 2008).

Total ammonia nitrogen is the combination of the ammonium ion (NH_4^+) and ammonia (NH_3). The amount of ammonium ion increases for lower pH, and the amount ammonia for higher levels of pH. At pH = 9.25, both forms are present in equal fractions.

The prevailing form of nitrogen in the water also gives the indication of the stage of pollution – in case of recent pollution, organic nitrogen and total ammonia are the most likely forms of nitrogen to be present. If the pollution is no longer recent, nitrate will be the prevailing form (Sperling 2008), in case O_2 is present.

2.2.4 Phosphorus

Phosphorus is an essential nutrient to microorganism growth and organic matter stabilization, being its main concern related to eutrophication of water bodies.

Similarly to nitrogen, phosphorus in domestic sewage takes form as organic and inorganic, being the second one originated from detergents and other household products and composed of polyphosphates and orthophosphates, while the organic fraction is originated physiologically. Furthermore, its classification can also be done according to its form as solids, where soluble phosphorus are mainly inorganic and particulate phosphorus are organic.

2.2.5 Microbiological contamination

Microbial contamination includes pathogenic organisms, which include bacteria, viruses, protozoans and helminths. These organisms are responsible for a number of diseases and several transmission mechanisms can take place: water borne, water hygiene, water based, water related. Contaminated water can contain human-specific enteric pathogens, such as *Salmonella*, hepatitis A and Norwalk-group viruses (Scott et al. 2002). Amongst a long list of potential diseases, the following can be highlighted: diarrhoea, fever, respiratory illness, vomiting and nausea.

The concentration of these pathogens is relatively low in the receiving water body, making it extremely difficult to measure. As a solution, indicator organisms are measured instead. These are predominantly non-pathogenic, and their presence indicates faecal contamination.

Total coliforms, TC, encompass bacteria that have been detected in water samples, polluted and non-polluted soils and plants, and human and non-human faeces. For this reason, TC are not a faecal contamination indicator but can still be used as a water treatment efficiency indicator, given that in drinking water, it is expected to find no TC at all.

Faecal coliform, FC, are present in the intestinal tract of humans and other animals and are discharged at a rate of 100 to 400 billion per day per person. High temperature destroys most bacteria of non-faecal origin. However, even in these conditions, the occurrence of non-faecal bacteria may still be possible, even if at smaller proportions. As a result, faecal coliform tests may not necessarily represent exclusive faecal contamination, and for this reason, the designation of thermotolerant coliforms has been instead adapted.

The main bacterium of the thermotolerant coliform are the *Escherichia coli*, EC, and their presence, which is tested with fluorogenic methods, guarantees exclusive faecal contamination. However, EC tests do not indicate if the contamination is human or animal.

Faecal streptococci is a group that includes the genera *Enterococcus* and *Streptococcus*. Many of the species of *Enterococcus* are of human origin and some of animal origin. The species *bovis* and *equinus* of the genus *Streptococcus* are abundant in animal faeces.

Clostridium perfringens may be found in faeces but in much lower quantities as *E. coli*. Even though these organisms may not be exclusively of faecal origin, their importance relies on the fact that they are extremely resistant to disinfection treatments and have the ability to survive to long periods of time. For these reasons, *C. perfringens* are on one hand good indicators of water disinfection efficiency, and on the other hand, reliable indicators of intermittent or remote contamination.

Bacteriophages are bacteria infecting viruses and are used for the detection of viruses. Bacteriophage are abundantly found in sewage, in spite of not being present in high number in human or animal faeces. This is for the fact that they are more resistant to treatment and reproduce at a fast rate, making them a valid treatment efficiency indicator.

Helminths do not have a replacing indicator and their eggs must be directly determined in laboratory tests. If water used for irrigation is contaminated, humans are exposed to helminths via direct contact or by ingestion of uncooked or unpeeled vegetables. In this sense, helminths are important for the assessment of the suitability of a certain treated water to be used for irrigation (Sperling 2008).

2.3 Pollutant removal mechanisms in TW

Unlike other conventional WWTP which require several reactors and unit operations, TW allow for a set of mechanisms to simultaneously take place in the same site. In general terms, TW clean the water that flows through them via mechanisms of sedimentation, filtration, flocculation, adsorption, in a physical-chemical manner, whilst simultaneously, biological action from the biofilm (which is part of the system) allows for biodegradation.

These physical, chemical and biological processes can be categorized by type of pollutant removed, as summarized in Table 1.

Table 1: Types of pollutants, main concerns and removal mechanisms in TW

	Main concerns	**Removal mechanism in TW** (Dotro et al. 2018)
Suspended solids, SS	Reduced light penetration in the water, T changes, clogging of channels and reservoirs. Chemical alterations which may lead to release of contaminants. DO depletion due to *in-situ* decomposition of SS with high OM content level (Bilotta and Brazier 2008)	Sedimentation and filtration.
Organic matter, OM	DO depletion. Some compounds may be toxic and biorefractory (Indian Institute of Tecnhology, n.d.).	Particulate OM: sedimentation and filtration. Dissolved OM: aerobic and/or anaerobic biodegradation. HFTW are more efficient compared to VFTW.
Nitrogen, N	Eutrophication. Algal blooms due to a high amount of nutrients cause DO depletion, may be toxic and cause harmful bacterial growth.	Ammonification-nitrification-denitrification, plant uptake and export through biomass harvesting. VFTW are more efficient compared to HFTW.
Phosphorus, P		Adsorption-precipitation carried out by substrate media, plant uptake and export through biomass harvesting.
Pathogens	Pathogenic bacteria are responsible for transmitting diseases such as typhoid fever and cholera (Sousa 2001).	Sedimentation, filtration, natural death decay, predation, UV degradation, adsorption.

2.3.1 Suspended solids removal

Depending on the type of TW – free water surface or subsurface flow – the mechanisms for removal of suspended solids take different forms. For FWS, the main processes that take place are flocculation-sedimentation and filtration-interception. Furthermore, in this type of TW, filtration mechanisms are not so relevant, when compared to SSF TW.

Settling by gravity – which is influenced by factors such as particle size and shape, by their specific gravity and by the properties of the fluid medium – is classified as discrete or flocculent. In the

first case, the particle settles individually, without attaching to any other particle, and its settling velocities can be fairly described by Newton's and Stokes' Laws. In contrast, flocculent settling happens when different particles associate, resulting in different sizes and characteristics. The bigger the dimensions of the particle or aggregate, the faster it settles: larger particles may be removed in the primary zones of the TW, while smaller particles are dependent on velocity gradients that result from he system's plant stems. Concerning filtration and interception, as mentioned before the first is not the most relevant in FWS TW, and the latter is possible because of the surface of the plants. The surface of such plants is coated with an active layer of biofilm which absorbs colloidal and suspended matter; later these solids may be metabolized and converted into gas or biomass (Norton 2003).

Different authors defend that 60-75% of the suspended solids in a SSFTW are retained on the first third of the system (Manios et al., 2003).

SSF TW are more efficient in removing suspended solids thanks to their large media surface area and low flow velocity. The mechanisms that take place are gravity settling, straining and adsorption onto gravel or plant media. Because media clogging by suspended solids is of concern in these systems, the type of filling media must be carefully selected upon the construction of the TW (Norton 2003).

2.3.2 Organic matter removal

The removal of this fraction is carried out by both physical processes, such as filtration and sedimentation, as well as by aerobic and anaerobic processes mediated by the microbial community (Vymazal and Kröpfelová 2009).

The physical mechanisms of removal are similar to those of suspended solids removal and apply to a fraction of the organic matter designated by particulate organic matter. Biodegradation is carried out by specific microorganisms and refers to the fraction of soluble organic matter (Dotro et al. 2018). The mentioned biodegradation is dependent on the on the attached and suspended microbial growth.

The composition of organic matter is 50% carbon, the energy source used by microorganisms. In the process of breaking down the organic molecules, the microbial population utilizes dissolved oxygen. Its quantities are measured through BOD, as seen previously (Norton 2003).

The majority of the microorganism-mediated reactions take place in aerobic, anoxic and anaerobic environments. Aerobic conditions are characterized by the presence of oxygen, which is used as the terminal electron acceptor. In the case of anoxic environments, the terminal electron acceptors are nitrates and nitrites. In anaerobic conditions, sulfates and carbonates are both the terminal electron acceptor as well as the donor (Norton 2003).

Aerobic processes

Aerobic degradation requires oxygen that is supplied to the water by diffusion from the atmosphere or by oxygen leakage from the plants' rhizosphere. The reaction between the organic matter and the oxygen will result in the production of carbon dioxide, water, electrons and energy, as described below (1):

$$C_6H_{12}O_6 + 6O_2 \rightarrow 6CO_2 + 6H_2O + \text{energy} \quad (1)$$

The type of microorganisms that carry out these reactions are aerobic heterotrophic bacteria (Vymazal et al. 1998). Ammonifying bacteria were also found to decompose organic matter containing nitrogen under these conditions. However, the rate at which the heterotrophs operate is superior enough to consider that these bacteria are responsible for the majority of BOD_5 reduction. In case oxygen supply to the system is not a limiting factor, it's the availability of organic matter that governs the performance of aerobic degradation. For this reason, in order to effectively remove organic matter, the TW must also have available organic matter to maintain the bacterial population responsible for its desired degradation.

Besides the heterotrophic and the ammonifying bacteria, there is another group which requires oxygen consumption – nitrifying bacteria. This group however is outcompeted by the heterotrophs (Vymazal 2005).

Aerobic oxidation releases great quantities of energy, allowing high growth rates to aerobic organisms. For this reason, in comparison to other oxidation conditions, this type of environment allows for a relatively large production of new cells (Mackenzie 2010).

Regarding the type of TW, for horizontal flow TW, oxygen is supplied by influent inputs, physical surface re-aeration and plant release. Concerning VF TW, the intermittent loadings are responsible for aerating the system, providing thus the oxygen necessary for aerobic degradation processes. For this reason, the prevailing organic matter removal mechanisms in VF TW are via aerobic processes.

Anaerobic processes

In the absence of oxygen, the anaerobic bacteria responsible for organic matter degradation perform in a multi-step process, including hydrolysis and fermentation followed by methanogenesis. The first step concerns the simplification of bigger organic molecules into more easily degradable monomers. The following step results in the conversion of the formed monomers into methane and carbon dioxide (Meng et al., 2014).

The initial fermentation reaction results in products such as acetic, butyric, and lactic acids (Eq. (2)), alcohols (Eq. (3)) and CO_2 and CH_4 gases (Eq. (4)).

$$C_6H_{12}O_6 \rightarrow 3CH_3COOH + H_2 \quad (2)$$

$$C_6H_{12}O_6 \rightarrow 2CH_3CHOHCOOH \text{ (lactic acid)} \quad (3)$$

$$C_6H_{12}O_6 \rightarrow 2CO_2 + 2CH_3CH_2OH \text{ (ethanol)} \quad (4)$$

The fermentation products will then follow one of two paths: either they are converted into CO_2 and CH_4, or the products are subjected to a process of acetogenesis. The microorganisms responsible for the second fermentation are strictly anaerobic sulfate-reducing (5) and methane-forming bacteria (6), (7) (Vymazal et al. 1998).

$$CH_3COOH + H_2SO_4 \rightarrow 2CO_2 + 2H_2O + H_2S \quad (5)$$

$$CH_3COOH + 4H_2 \rightarrow 2CH_4 + 2H_2O \quad (6)$$

$$4H_2 + CO_2 \rightarrow 2CH_4 + 2H_2O \quad (7)$$

2.3.3 Nitrogen removal

In TWs, the removal of nitrogen compounds is possible by physicochemical and biological processes, as well as through plant uptake. The physicochemical processes include adsorption and sedimentation. Regarding the biological processes, these could be either carried out via classic routes – ammonification, nitrification and denitrification – or via Annamox routes – anaerobic ammonium oxidation. Plant uptake concerns the macrophytes use of nutrients for their growth and maintenance.

Nitrogen biodegradation – classic routes

The typical sequence of reactions for nitrogen removal is given by ammonification, nitrification and denitrification, where in the first step organic nitrogen is converted into ammonia (8), after which, ammonia volatilization converts ammonia NH_3 into ammonium ion NH_4+ (9), ready to be used in the nitrification step. In this reaction, two consecutive steps transform the ammonium ion into nitrite (10) and nitrite into nitrate (11), and lastly, nitrate is transformed into gaseous N_2, ready to be safely released back into the atmosphere (12) (Lee et al., 2009).

$$R\text{-}NH_2 \rightarrow NH_3 \quad (8)$$

$$NH_3(aq) + H_2O \rightarrow NH_4^+ + OH^- \quad (9)$$

$$NH_4^+ + 3/2O_2 \rightarrow NO_2^- + H_2O + 2H^+ \quad (10)$$

$$NO_2^- + 1/2O_2 \rightarrow NO_3^- \quad (11)$$

$$6(CH_2O) + 4NO_3^- \rightarrow 6CO_2 + 2N_2 + 6H_2O \quad (12)$$

In the process of ammonification, which is kinetically faster than nitrification, the rates are higher in oxygenated zones than in other areas, with microorganisms switching from aerobic to facultative or obligate anaerobes. Other factors which influence the rate of ammonification comprehend pH, temperature, carbon to nitrogen (C/N) ratio, nutrient availability and soil structure (Vymazal 2007).

As far as nitrification is concerned, the microorganisms involved in the first step of conversion of ammonia to nitrite are strictly aerobic bacteria, such as *Nitrosomonas*, while nitrite conversion into nitrate is mediated by bacteria such as *Nitrobacter*. Because autotrophic nitrifying bacteria have much lower respiration rates than BOD removal heterotrophs, significant nitrification in SSF TW won't take place until a substantial BOD removal. On the other hand, factors which influence the rate of nitrification include temperature, pH, alkalinity, inorganic carbon source, moisture, microbial population, ammonium-N concentration and DO concentration (Lee, Fletcher, and Sun 2009). The irreversible reaction of denitrification occurs only in anoxic conditions and is carried out by heterotrophs and autotrophs.

2.3.4 Phosphorus removal

In wastewaters, the most common forms of phosphorus are as orthophosphates (which can be resultant from biological oxidation), and other inorganic phosphorus forms (Vymazal et al. 1998). The main mechanisms of removal are through adsorption-precipitation and uptake from plant roots and microorganisms. The first type of mechanism concerns inorganic phosphorus removal, which is carried out by its movement from the soil surface to the soil media pores. The adsorption quality of the soil increases with the increase of its clay content. The main issue with this process is that the storage in soil media or plant tissue is limited and once it reaches maximum capacity the mechanism is no longer possible. As far as uptake from plants and microorganisms, it is relevant to mention that the storage capacity depends on the type of plant and is generally longer below the ground than it is above it. Finally, phosphorus uptake by microorganisms is faster than by plants, given that bacteria fungi and algae multiply quickly. However, their storage capacity is limited.

In SSF TW (with emerged plants), the most efficient removal mechanism for phosphorus is by soil adsorption. It is necessary to take into consideration that the type of filling media of the TW will influence its phosphorus storage capacity. As far as FWS TW, the free floating macrophytes are the ones mainly responsible for the removal. These must however be periodically harvested and replaced in order to maximize the process.

2.3.5 Pathogen removal

Pathogen removal is of extreme importance, given the threat they represent to public health.

The main pathogen removal mechanism by TW is sedimentation: it was found that river mud contains 100-1000 times more faecal contamination than surface water. On the other hand, filtration by plant root structure is also thought to be a removal mechanism (Norton 2003). Antibiosis, predation by other organisms and natural die-off are the typical biological routes for pathogen removal (Vymazal et al. 1998).

2.4 Measuring and modelling biodegradation

2.4.1 The need for models

The materialization of an engineering construction requires detailed planning before investing the necessary financial, human and time resources, as well as materials and tools. Several factors must be carefully assessed *a priori*, from safety to efficiency, in order for a certain project to fulfill the desired tasks. In waste water treatment, such planning is made possible via models, which are in constant development, bringing newer and more robust knowledge each decade. The ways in which Nature works are sought to be translated into processes, components and parameters which can be manipulated mathematically, allowing for ever more accurate predictions. Models are in one hand used to predict but also to understand several mechanisms involved in a certain process, given that it is not possible to measure everything.

2.4.2 Activated sludge models

Since its first application in the 1920's, the activated sludge process has been extensively used around the world as a biological wastewater treatment process. In general terms, this chain of processes involves the development of microorganisms that feed on the carbonaceous matter from the wastewater.

The activated sludge is a mass formed by amalgamated microorganisms attached between them by a secretion of adhesive substances, resulting in a structure designated as biofloc. These substances are secreted by the microorganisms themselves and produce a slime or gel containing enzymes that allow for the break-down of bigger organic molecules. The types of bacteria that populate an activated sludge are mainly heterotrophs, which feed on organic molecules, and nitrifying bacteria, which in turn feed on inorganic chemicals.

Aeration must be ensured so that dissolved oxygen is supplied for the microorganisms to degrade the organic matter, and for nitrification to occur. On the other hand, the period of time in which the activated sludge is in contact with the sewage – the retention time – must also be sufficient for the reactions to take place (Ahansazan et al. , 2014).

Biokinetic parameters, stoichiometric coefficients and activated sludge models

The design of WWTP was traditionally carried out based on empirical data sets such as hydraulic, organic loadings and retention times. More recently, the assessment of biokinetic parameters has been the used approach, given that it allows the prediction of the biological processes which govern the microbes responsible for wastewater treatment. These processes include for instance microbial growth, substrate utilization rates, food-to-microorganism ratio and mean cell residence time (Mardani et al., 2011).

The evolving approaches have throughout the last two decades moved towards a more holistic overview of biological processes, paying close attention to chemistry, mathematics, microbiology, physical and bioprocess engineering, to a point where predictions have been coded as mathematical models (Van Loosdrecht et al., 2015).

The uniformization of the models developed around the world was first materialized as the Activated Sludge Model 1, ASM1, in 1987 (Jeppsson 1996).

As the model became more and more applied throughout the years, several constraints were encountered and solved, giving way to the evolution from ASM1 to ASM3.

Brief description of the Activated Sludge Model 1, ASM1

In order to have a fair understanding of how respirometry works, it is pertinent to start by introducing the biokinetic processes that take place in microbe-mediated water treatment, as well as the variables that define them.

In 1983, a task group was formed by the International Association on Water Quality, IAWQ, to uniformize the work developed around the world in modelling and design for WWT systems. And so, in 1987 the group introduced the ASM1, in which state variables such as COD, nitrogen and other

components were described, followed by the dynamic processes, the model parameters and its equations and restrictions (Jeppsson 1996). The model was based on Monod kinetics for prediction of the processes of biological reactions.

These pieces were all put together in a matrix. The purpose of the model is to model COD and N removal, as well as oxygen consumption and sludge production (Van Loosdrecht et al. 2015).

The ASM1 was then established with 13 components and 8 reactions. In general terms, the components are classified according to solubility (particulate X, soluble S), biodegradability, biodegradation rate and viability of each fraction. The fractions are of COD and N, and their viability refers to the portion that results in biomass (active mass). COD is defined by seven parameters, whilst N by 4 parameters (Petersen et al., 2003).

ASM1 components: COD, nitrogen and others

Given that carbonaceous material is the main source used by the heterotrophic biomass – which includes bacteria and their storage material, as well as protozoa and other higher organisms – to obtain energy, the model will firstly define all possible COD forms, which in this context represents organic matter (Vanrolleghem 2002).

Total COD is the sum of three fractions: the biodegradable, the non-biodegradable and the biomass itself (active mass). In order to further divide these three COD classes, the concept of particulate (X) and soluble (S) arises. In fact, each of the branches just mentioned are further divided into soluble biodegradable COD, which is readily biodegradable substrate, and particulate biodegradable COD, which is slowly biodegradable substrate, soluble inert COD (inert meaning non-biodegradable) and particulate inert COD, and concerning the biomass, it is divided into autotrophs or heterotrophs.

The inert fraction of COD sees two fates: whilst the soluble fraction S_I is removed in the secondary clarifier effluent of the WWTP, the particulate inert material X_P will integrate with the sludge mass and accumulate as inert volatile suspended solids, VSS. There is another component which is a part of particulate inert COD – the product of biomass decay, expressed as X_P (Jeppsson 1996).

The readily biodegradable fraction S_S is composed of relatively simple molecules which heterotrophs directly take for growth and for new biomass. The slowly biodegradable fraction of COD, X_S is in turn composed by more complex molecules, which require enzymatic breakdown before utilization. It is also worthy of note that some of X_S may actually be soluble (Petersen and Gernaey 2003). Finally, the COD classification can be abbreviated into the following equation:

$$COD_{Tot} = S_I + S_S + X_I + X_S + X_{BH} + X_{BA} + X_P \quad (13)$$

Concerning nitrogen, total N is given by the sum of total Kjeldahl N (TKN) and nitrate + nitrite (S_{NO}). As Table 2 shows, the classification of N parameters in ASM1 is fairly similar to that of COD. The total nitrogen according to ASM1 is the result of the equation 14:

$$N_{Tot} = S_{NO} + S_{NH} + S_{ND} + X_{ND} \quad (14)$$

In order to complete the description of the biokinetic processes two more components were introduced in ASM1: negative COD given by dissolved oxygen concentration, S_O, and alkalinity, S_{ALK} (Jeppsson 1996). Table 2 summarizes the components in ASM1.

Table 2: ASM1 components, adapted from Activated Sludge Model no. 1

	COD components	
S_I	Soluble inert organic matter	[M(COD) L^{-3}]
S_S	Readily biodegradable substrate	[M(COD) L^{-3}]
X_I	Particulate inert organic matter	[M(COD) L^{-3}]
X_S	Slowly biodegradable substrate	[M(COD) L^{-3}]
$X_{B,H}$	Active heterotrophic biomass	[M(COD) L^{-3}]
$X_{B,A}$	Active autotrophic biomass	[M(COD) L^{-3}]
X_P	Particulate material from biomass decay	[M(COD) L^{-3}]
	Nitrogen components	
S_{NO}	Nitrate and nitrite nitrogen	[M(N)L^{-3}]
S_{NH}	Ammonia and ammonium nitrogen	[M(N)L^{-3}]
S_{ND}	Soluble biodegradable organic nitrogen	[M(N)L^{-3}]
X_{ND}	Particulate biodegradable organic nitrogen	[M(N)L^{-3}]
	Other components	
S_O	Oxygen (negative COD)	[M(-COD)L^{-3}]
S_{ALK}	Alkalinity	[molar units]

Processes in ASM1

The 8 processes described by the model (Table 3) are based on the following four main processes: growth and decay of biomass, ammonification of organic nitrogen and hydrolysis of particulate matter entrapped in the biofloc.

Table 3: ASM1 processes, adapted from Activated Sludge Model no. 1 (Henze, M. 1987)

Biomass growth	Aerobic growth of heterotrophic biomass
	Anoxic growth of heterotrophic biomass (denitrification)
	Aerobic growth of autotrophic biomass (nitrification)
Biomass decay	Decay of heterotrophic biomass
	Decay of autotrophic biomass
Ammonification	of soluble organic nitrogen
Transformation	Hydrolysis of entrapped organics
	Hydrolysis of entrapped organic nitrogen

Stoichiometric and kinetic parameters in ASM1

19 parameters were compiled to better characterize the processes that take place, of which 14 are kinetic and the remaining 5 are stoichiometric (Table 4).

Table 4: ASM1 stoichiometric and kinetic parameters, adapted from Activated Sludge Model no. 1 (Henze, M. 1987)

	Stoichiometric parameters
Y_H	Yield of heterotrophic biomass on S_S
Y_A	Yield of autotrophic biomass on S_{NH}
f_P	Fraction of biomass yielding particulate products
$i_{X,B}$	Mass N/mass COD in biomass
$i_{X,P}$	Mass N/mass COD from biomass particulate products
	Kinetic parameters
$\hat{\mu}_H$	Heterotrophic maximum specific growth rate
K_S	Half-saturation coefficient for heterotrophs
$K_{O,H}$	Oxygen half-saturation coefficient for heterotrophs
K_{NO}	Nitrate half-saturation coefficient for denitrifying heterotrophs
b_H	Heterotrophic decay rate
$\hat{\mu}_A$	Autotrophic maximum specific growth rate
K_{NH}	Ammonia half-saturation coefficient for autotrophs
$K_{O,A}$	Oxygen half-saturation coefficient for autotrophs
b_A	Autotrophic decay rate
η_g	Correction factor for anoxic growth of heterotrophs
k_A	Ammonification rate
k_h	Maximum specific hydrolysis rate
K_X	Half-saturation coefficient for hydrolysis of slowly biodegradable substrate
η_h	Correction factor for anoxic hydrolysis

Furthermore, it was established that the value for a certain number of parameters and characteristics could be assumed (such as Y_A and b_A) while others had to be estimated and required other information for their evaluation (like Y_H and b_H). In a subchapter dedicated to default values, the ASM1 made available a set of typical parameter values at neutral pH, at 20ºC and 10ºC. Moreover, a table is also given for typical characteristics of settled domestic sewage in Denmark, Switzerland and Hungary. Table 5 contains some of these typical values for the parameters of interest in the context of this work, as well as the component of interest S_S with the typical values for each of the stated countries.

Table 5: ASM1 typical parameter values (at 10ºC and 20ºC) and S_S component value for Denmark, Switzerland and Hungary, adapted from Activated Sludge Model no. 1 (Henze, M. 1987)

Parameter	**Unit**	**Value at 10ºC**		**Value at 20ºC**
Y_H	g cell COD formed (g COD oxidized)$^{-1}$	0,67		0,67
b_H	day^{-1}	0,20		0,62
Component	**Unit**	**Denmark**	**Switzerland**	**Hungary**
Ss	g COD m^{-3}	125	70	100

ASM1 limitations and its evolution into ASM2, ASM2d and ASM3

At the time of the development of ASM1, WWTPs did not incorporate biologically or chemically enhanced phosphorus removal technologies, even though knowledge on enhanced biological phosphorus removal (EBPR) processes was already existent. Instead, this model only described heterotrophic and autotrophic reactions under aerobic and anoxic conditions. As a response to this limitation, the ASM2 was presented in 1990, including phosphate accumulating organisms (PAO). These organisms which grow only under aerobic conditions were characterized with their corresponding anaerobic, anoxic, and aerobic reactions.

In order to include the process of denitrification in EBPR, a new version of ASM2 called ASM2d was presented in 1999, where denitrifying PAO (DPAO) were included.

Parallel to the publication of the ASM2d, other deficiencies of the ASM1 were corrected, resulting in the ASM3, which was proposed to become the new standard for ASM-based modelling.

Brief description of the Activated Sludge Model 3, ASM3

Following the advances presented by both ASM2 and ASM2d, important breakthroughs were possible thanks to the ASM3. Maintaining the structure and description of its precedent models, it allowed describing three different rates of oxygen-consuming process. Furthermore, it allowed for the definition of a storage compound that would explain the difference in mechanisms of bacterial consumption and storage, in case of periodical shortage of substrate (Henze et al., 2000).

The novelty of ASM3 – storage and oxygen consumption rates

Besides correcting some shortcomings from ASM1, one of the main novelties the ASM3 presented has to do with the introduction of a storage compound, $X_{STO,S}$, which allowed explaining the observations in oxygen uptake rate (OUR) tests. When a defined substrate, like acetate, was added to the activated sludge, the OUR would indicate the presence of two substrates. This is due to the fact that bacteria were taking-up rapidly biodegradable COD (defined as S_S in ASM1) and storing it as an internal substrate. This latter would then be slowly converted (X_S, according to ASM1). The constraint of this phenomena through the lens of ASM1 is that only one substrate was added, the S_S, but two were observed – the S_S and the X_S. In order for this to fit the ASM1 principles, it would be necessary to define

the acetate as partly soluble and partly particulate. By introducing the component of $X_{STO,S}$, the ASM3 was able to explain that the added substrate would first be rapidly taken-up and stored, after which bacterial growth would occur on the stored substrate. Although both models are able to describe the mentioned OUR, only ASM3 could accurately describe the uptake.

Another very important evolution the new model brought has to do with oxygen consumption rates: while ASM1 described only one oxygen-consuming process, the ASM3 proposed three rates: a rapid rate of oxygen consumption for rapidly biodegradable COD, a slower rate for consumption of slowly biodegradable COD and finally, the slowest rate for endogenous maintenance of bacterial life. By replacing the decay process of ASM1 by endogenous respiration, the ASM3 was also able to eliminate the COD cycle. The issue of COD cycling proposed by ASM1 is that if in the decay process particulate COD is produced, hydrolyzed and used for growth again, it would mean that a change in one parameter in the process would imply changing all of the other processes, making calibration very difficult (Van Loosdrecht et al. 2015).

For a better viewing of the evolution in substrate flows between the two models, the diagram in

Figure 1 was elaborated based on the flow charts from (Gernaey et al., 2004) and (Henze et al. 2000).

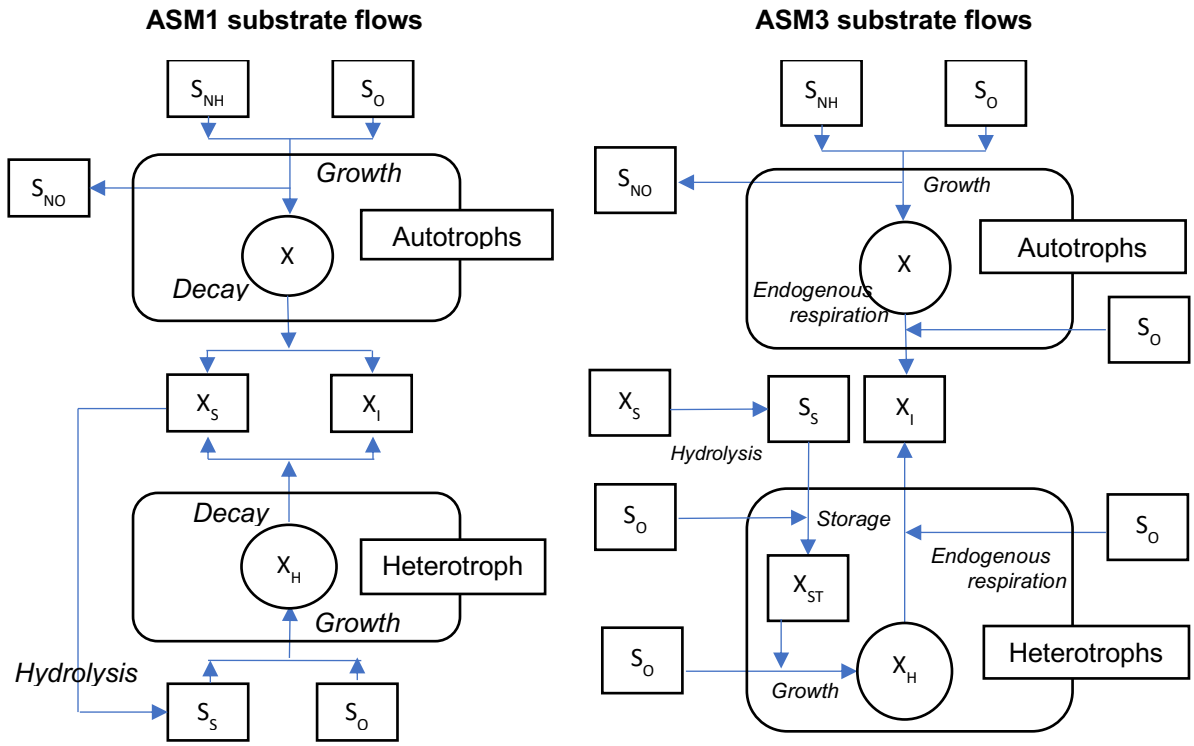

Figure 1: ASM1 and ASM3 substrate flows adapted from ASM3 (Henze et al. 2000)

ASM3 components

The components of ASM3 are given by Table 6, which separates soluble form particulate components, were the items in bold are the novelty compared to ASM1:

Table 6: ASM3 components, adapted from Gujer et al., 1999

	Soluble components, $S_?$	
S_I	Soluble inert organic matter	[M(COD) L^{-3}]
S_S	Readily biodegradable substrate	[M(COD) L^{-3}]
S_{NOX}	Nitrate and nitrite nitrogen	[M(N)L^{-3}]
S_{NH4}	Ammonia and ammonium nitrogen	[M(N)L^{-3}]
S_{N2}	**Dinitrogen**	[M(N) L^{-3}]
S_O	Dissolved oxygen (negative ThOD)	[M(O_2)L^{-3}]
S_{ALK}	Alkalinity of waste water	[mole(HCO_3)L^{-3} units]
	Particulate components, $X_?$	
X_I	Particulate inert organic matter	[M(COD) L^{-3}]
X_S	Slowly biodegradable substrate	[M(COD) L^{-3}]
X_H	Heterotrophic organisms	[M(COD) L^{-3}]
X_A	Nitrifying organisms	[M(COD) L^{-3}]
X_{STO}	**A cell internal storage product of heterotrophic organisms**	[M(COD) L^{-3}]
X_{SS}	Suspended solids	[M(SS) L^{-3}]

X_{STO} only occurs associated with it X_H but it is not included in its mass. It is a functional compound required for modelling, however it does not allow for the direct chemical identification of products stored by the cell, like poly-hydroxy-alkanoates (PHA) and glycogen. X_{STO} is assumed to have the chemical composition of poly-hydroxy-butyrate $(C_4H_6O_2)_n$, for stoichiometric considerations (Henze et al. 2000).

Processes in ASM3

There are 9 defined processes in this model (Table 7), which present some differences in comparison to ASM1. The importance given to the process of hydrolysis in the ASM1 is reduced in ASM3. On the other hand, the definition of cell inert storage processes allows describing the decay processes adapted to the environmental conditions. Finally, degradation of soluble and particulate organic nitrogen was integrated in the processes of hydrolysis, growth and decay (Henze et al. 2000).

Table 7: ASM3 processes, adapted from Activated Sludge Models ASM1, ASM2, ASM2d and ASM3 (Henze et al. 2000)

Transformation	Storage	Growth	Respiration
Hydrolysis	Aerobic storage of S_S in the form of X_{STO} Anoxic storage of S_S in the form of X_{STO}	Aerobic growth of X_H Anoxic growth of X_H	Aerobic endogenous respiration Anoxic endogenous respiration Aerobic respiration of X_{STO} Anoxic respiration of X_{STO}

2.4.3 The Simultaneous Storage and Growth model, SSAG

Biomass exposed to a real wastewater will come across different substrates with different concentrations. Its response is translated into two opposite conditions: feast and famine. In the first case, the biomass has access to external substrate in excess, whilst in the latter the substrate is absent. As described, the ASM3 attempted at explaining a storage mechanism in which in feast conditions readily biodegradable COD (S_S) would directly be converted into storage material, X_{STO}. In 1999, Krishna and Van Loosdrecht developed the Simultaneous Storage and Growth (SSAG) model (Figure 2), as an extension to the ASM3, with the purpose of better explaining the process of organic carbon oxidation in an activated sludge system (Hoque 2010). In the SSAG model, all of it components are similar to those of the ASM3.

In 2005, Sin et al. proposed and tested an adaptation of the SSAG model, in which the task of estimating stoichiometric parameters was significantly simplified. The proposed model and its calibration can be found further ahead, on subchapter 2.5.3, where the main procedures, results and conclusions of this research are further explained.

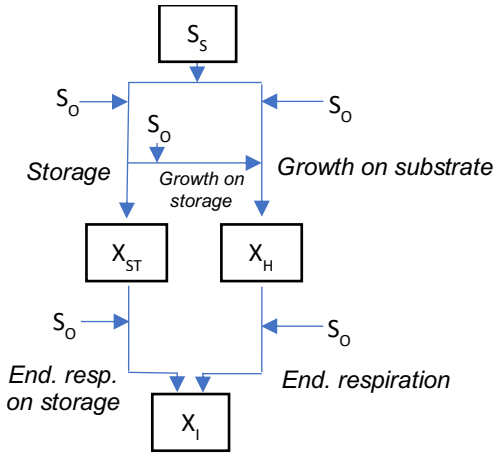

Figure 2: SSAG phenomena adapted from Hoque (2010)

2.4.4 Constructed Wetland Model 1, CWM1

Keeping in mind that some biological processes in TWs can be compared to those of activated sludge processes, adapting the IAWQ's ASMs into the desired context of TW modelling resulted in the work of Langergraber et al. in 2009: the Constructed Wetland Model No1, CWM1. The description of 17 processes and 16 components – 8 particulate and 8 soluble – aims to predict effluent concentrations from TW, without predicting gaseous emissions. Until 2009, several other models had been presented to describe the treatment capacity of TW, and it was their discussion and reformulation that originated the CWM1.

According to the authors, the CWM1's notation and structure is similarly described as in the ASMs, and like Henze, the authors' objective is to provide a widely accepted model for processes of biochemical transformation and degradation in TWs to be implemented in various simulation tools.

CWM1 components: soluble and particulate

The CWM1 describes its 16 components according to their solubility (Table 8). These include COD, N and oxygen, and introduce sulphur components. All microorganisms are classified as particulate and are referred to as bacteria, and organic nitrogen is considered as a fraction of COD.

Table 8: CWM1 components, adapted from Langergraber et al., 2009

	Soluble components, $S_?$	
S_O	Dissolved oxygen	[M(O_2) L^{-3}]
S_F	Fermentable, readily biodegradable soluble COD	[M(COD) L^{-3}]
S_A	Fermentation products as acetate	[M(COD) L^{-3}]
S_I	Inert soluble COD	[M(COD) L^{-3}]
S_{NH}	Ammonium and ammonia nitrogen	[M(N) L^{-3}]
S_{NO}	Nitrate and nitrite nitrogen	[M(N) L^{-3}]
S_{SO4}	Sulphate sulphur	[M(S) L^{-3}]
S_{H2S}	Dihydrogensulphide sulphur	[M(S) L^{-3}]
	Particulate components, $X_?$	
X_S	Slowly biodegradable particulate COD	[M(COD) L^{-3}]
X_I	Inert particulate COD	[M(COD) L^{-3}]
X_H	Heterotrophic bacteria	[M(COD) L^{-3}]
X_A	Autotrophic nitrifying bacteria	[M(COD) L^{-3}]
X_{FB}	Fermenting bacteria	[M(COD) L^{-3}]
X_{AMB}	Acetotrophic methanogenic bacteria	[M(COD) L^{-3}]
X_{ASRB}	Acetotrophic sulphate reducing bacteria	[M(COD) L^{-3}]
X_{SOB}	Sulphide oxidising bacteria	[M(COD) L^{-3}]

Processes in CWM1

These include processes of transformation, growth and lysis of bacteria (Table 9). Hydrolysis is the conversion of slowly biodegradable organic matter X_S into readily biodegradable organic matter S_F, with a small fraction being converted into inert organic matter S_I. It is performed by heterotrophs and fermenting bacteria, the latter assumed to be slower. It is further assumed that this process does not take place under direct dependence of the oxygen conditions.

Table 9: CWM1 processes, adapted from Langergraber et al., 2009

Transformation
Hydrolysis
Growth
Aerobic growth of heterotrophic bacteria on S_F
Aerobic growth of heterotrophic bacteria on S_A
Anoxic growth of heterotrophic bacteria on S_F
Anoxic growth of heterotrophic bacteria on S_A
Aerobic growth of autotrophic nitrifying bacteria on S_{NH}
Growth of fermenting bacteria
Growth of acetotrophic methanogenic bacteria
Growth of acetotrophic sulphate reducing bacteria
Aerobic growth of sulphide oxidising bacteria on S_{H2S}
Anoxic growth of sulphide oxidising bacteria on S_{H2S}
Lysis
Lysis of heterotrophic bacteria
Lysis of autotrophic nitrifying bacteria
Lysis of fermenting bacteria
Lysis of of acetotrophic methanogenic bacteria
Lysis of acetotrophic sulphate reducing bacteria
Lysis of sulphide oxidising bacteria

Stoichiometric and kinetic parameters in CWM1

The CWM1 presents a stoichiometric matrix based on the IWA ASM mathematical formulation by Henze et al., (2000), as well as their process rates, which are not given here, due to their extension. The stoichiometric parameters for this model are presented in Table 10, for organic matter and bacteria.

Table 10: CWM1 stoichiometric parameters for organic matter and bacteria, adapted from Langergraber et al., 2009

$f_{Hyd,SI}$	Production of S_I in hydrolysis	[$gCOD_{SI}/gCOD_{XS}$]
$f_{BM,SF}$	Fraction of S_F generated in biomass lysis	[$gCOD_{SF}/gCOD_{BM}$]
$f_{BM,XI}$	Fraction of X_I generated in biomass lysis	[$gCOD_{XI}/gCOD_{BM}$]
Y_H	Yield coefficient for heterotrophic bacteria	[$gCOD_{BM}/gCOD_{SF}$]
Y_A	Yield coefficient for autotrophic bacteria	[$gCOD_{BM}$/g N]
Y_{FB}	Yield coefficient for fermenting bacteria	[$gCOD_{BM}$/g COD_{SF}]
Y_{AMB}	Yield coefficient for acetotrophic methanogenic bacteria	[$gCOD_{BM}/gCOD_{SA}$]
Y_{ASRB}	Yield coefficient for acetotrophic sulphur reducing bacteria	[$gCOD_{BM}/gCOD_{SA}$]
Y_{SOB}	Yield coefficient for sulphide oxidizing bacteria	[$gCOD_{BM}$/gS]

In Table 11, some typical values are presented, which can be compared to those presented previously for ASM1 in Table 5.

Comparing to the typical values suggested in the ASM1 for Y_H, 0,67, the one for CWM1 is very similar. As far as the values proposed for b_H, it coincides at 10ºC but it is lower at 20ºC, compared to the ASM1 value: 0,62.

Table 11: CWM1 typical parameter values (at 10ºC and 20ºC), adapted from Langergraber et al., 2009

Parameter	**Unit**		
Y_H	[$gCOD_{BM}/gCOD_{SF}$]	0,63	
Parameter	**Unit**	**Value at 10ºC**	**Value at 20ºC**
b_H	day^{-1}	0,20	0,40

The extension of the biokinetics and stoichiometry of the CWM1 indicate how much more complex and difficult to predict the bioprocesses that take place in a TW are, when compared to those of an activated sludge. It is notable how for the CWM1 there are parameters for 6 types of bacteria, when in ASM these are only discriminated for autotrophic and heterotrophic bacteria.

Table 12 summarizes the kinetic parameters of the CWM1.

Table 12: Synthesis of kinetic parameters in CWM1, adapted from CWM1

	Hydrolysis rate constant K_h	**Correction factor for hydrolysis by fermenting bacteria** η_H	**Correction factor for denitrification by heterotrophs** η_g	**Saturation/ inhibition coefficients** $K_?$	**Maximum aerobic growth rate** $\eta_?$	**Rate constant for lysis** $b_?$
Hydrolysis	x	x		x	x	
Heterotrophic bacteria (aerobic growth and denitrification), $?_H$			x	x	x	x
Autotrophic bacteria, $?_A$				x	x	x
Fermenting bacteria, $?_{FB}$				x	x	x
Acetotrophic methanogenic bacteria, $?_{AMB}$				x	x	x
Acetotrophic sulphate reducing bacteria, $?_{ASRB}$				x	x	x
Sulphide oxidising bacteria, $?_{SOB}$				x	x	x

2.5 Respirometry as an information supply tool for modelling

2.5.1 Brief description of the tool

The measurement and interpretation of biological oxygen consumption rate under well-defined experiments is a procedure known as respirometry. Its initial application was developed in the scope of activated sludge processes, for monitoring, modelling and control. In the early stages of its application, respirometry was used as a substitute to traditional BOD tests. As of the last decade, it has been increasingly explored for obtaining biokinetic characteristics in order to better model biological processes. Respirometry measures the respiration rate of the given subject under study.

The respiration rate is defined as that at which the microorganisms consume oxygen to breakdown organic molecules, and its measurement is carried out by a tool called respirometer (Vanrolleghem 2002). Furthermore, the respiration rate is of great interest, given that it allows to directly link oxygen uptake to substrate removal as well as to biomass growth (IAWQ, 1998).

The reactor is a component common to every respirometer, except for when the aeration tank of the WWTP is the respirometer itself. The different components, such as biomass and substrate, are all combined in the reactor.

As explored in the past, respirometry is a useful technique for the assessment of kinetic parameters and stoichiometric coefficients (Spanjers et al., 1995).

The following description of the tool is as proposed by the IWAQ in the 1996 Scientific and Technical Report (STR) on Respirometry in Control of the Activated Sludge Process.

Biochemical background to explain respirometry

The aerobic respiration measured by the respirometers can be explained as a chain of processes:

1) Obtaining energy to transform into ATP – organic substrate contains energy in its intramolecular bonds, which the bacteria convert into the high energy phosphate bonds of adenosine triphosphate, ATP.

2) Converting energy into ATP – a series of oxidation-reduction processes take place. The electrons are removed from the organic substrate via oxidation; these electrons are then transferred along an electron transport chain to their terminal acceptor, the oxygen, under a reaction defined as aerobic respiration.

3) ATP as a source for molecular components – the energy in ATP obtained from the organic substrate bonds is used to synthesize the components necessary for cell growth and reproduction (IAWQ, 1998).

2.5.2 Measuring Principles

Types of respirometers

This section was developed based mostly on (Henri Spanjers, Vanrolleghem, and Ekama 2016) and (Vanrolleghem 2002). According to the measuring technique, respirometers can be classified according to two main groups: the type of phase where the concentration of oxygen is measured – liquid or gas – and the presence or absence of input and output of liquid and gas – flowing or static. Figure 3 illustrates the generic setup of a respirometer.

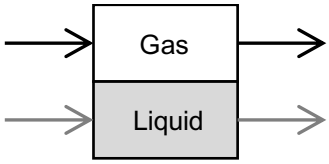

Figure 3: Generic setup of a respirometer

The different mass balances distinguish the 8 possible types of respirometers. Taking as a starting point both the DO mass balance over the liquid phase (Eq. 15) and the oxygen mass balance over the ideally mixed gas phase (Eq. 16), it is possible to analyze each term as a different process.

$$\frac{d(V_L S_O)}{dt} = \underbrace{Q_{in}S_{O,in} - Q_{out}S_O}_{\text{liquid flow}} + \underbrace{V_L K_L a(S_O^* - S_O)}_{\text{interface exchange}} - \underbrace{V_L r_O}_{\text{respiration}} \quad (15)$$

$$\frac{d(V_G C_O)}{dt} = \underbrace{F_{in}C_{O,in} - F_{out}C_O}_{\text{gas flow}} - \underbrace{V_L K_L a(S_O^* - S_O)}_{\text{interface exchange}} \quad (16)$$

S_O	DO concentration in the liquid phase (mg L^{-1})	V_L	Volume of the liquid phase (L)
S_O^*	Saturation DO concentration in the liquid phase (mg L^{-1})	C_O	O_2 concentration in the gas phase (mg L^{-1})
$S_{O,in}$	DO concentration in the liquid phase entering the system (mg L^{-1})	$C_{O,in}$	O_2 concentration in the gas entering the system (mg L^{-1})
$K_L a$	Oxygen mass transfer coefficient (based on liquid volume) (h^{-1})	F_{in}	Flow rate of the gas entering the system (L h^{-1})
Q_{in}	Flow rate of the liquid entering the system (L h^{-1})	F_{out}	Flow rate of the gas exiting the system (L h^{-1})
Q_{out}	Flow rate of the liquid exiting the system (L h^{-1})	V_G	Volume of the gas phase (L)
r_O	Respiration rate of the biomass in the system (mg L^{-1} h^{-1})		

Measuring oxygen in the liquid phase

The respirometers in which oxygen is measured in the liquid phase include four types of setups:

- Static gas – static liquid, LSS
- Flowing gas – static liquid, LFS
- Static gas – flowing liquid, LSF
- Flowing gas – flowing liquid, LFF

Their respective characteristics, mass balances and main advantages and disadvantages, as well as a schematic representation can be found in Table 13.

Table 13: Types of liquid phase respirometers and main considerations

Static gas – static liquid, LSS

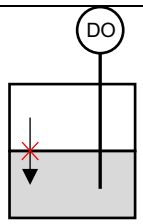

$$\frac{d(S_O)}{dt} = -r_O \approx \frac{\Delta S_O}{\Delta t} = -r_O \quad (17)$$

No liquid flow and no oxygen mass transfer.

Respiration rate r_O determination: measuring the decrease in DO as a function of time. Base principle for r_O determination according to Standard Methods of the American Public Health Association (1992).

Advantages: requires only DO concentration recordings.

Disadvantages: reaeration is necessary to bring up DO concentrations, given that it may become exhausted after some time. Complications in the assessment of the differential term arise because DO and substrate at low concentrations cause a non-linear DO decrease.

Flowing gas – static liquid. LFS

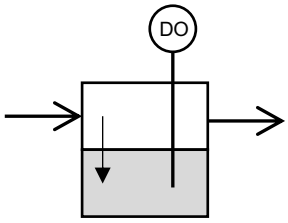

$$\frac{d(S_O)}{dt} = K_L a(S_O^* - S_O) - r_O \quad (18)$$

Continuous biomass aeration.

Respiration rate r_O determination: the mass transfer coefficient $K_L a$ and the DO saturation concentration S_O^* must be known. Their estimation can be either done by using separated reaeration tests and look-up tables, or by applying parameter estimation techniques.

Advantages: The values of the aeration coefficients can be updated easily, for the parameter estimation.

Static gas –flowing liquid. LSF

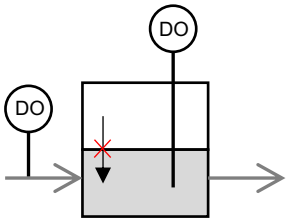

$$\frac{d(S_O)}{dt} = \frac{Q_{in}S_{O,in}}{V_L} - \frac{Q_{out}S_O}{V_L} - r_O \quad (19)$$

It is the continuous counterpart of the LSS. A liquid with a high enough input DO concentration flows continuously through a completely mixed closed cell, with no gas phase.

Respiration rate r_O determination: DO, $S_{O,in}$ and S_O must be measured. Q_{in} and V_L are instrument constants.

Disadvantages: as the LSS, it is also sensitive to the effect of substrate and DO limitation.

Advantages: the limiting effect of DO and biomass can be eliminated by continuously supplying substrate (in the form of wastewater) and DO to the respiration cell.

Table 13: Types of liquid phase respirometers and main considerations (cont.)

Flowing gas – flowing liquid. LFF	
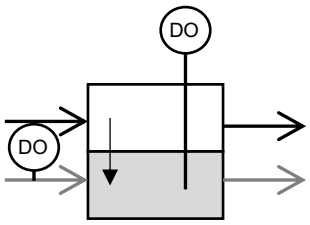 $\frac{d(V_L S_O)}{dt} = Q_{in} S_{O,in} - Q_{out} S_O + V_L K_L a(S_O^* - S_O) - V_L r_O$ (20)	Full mass balance, with no simplifications. Respiration rate r_O determination: requires a combination of the approaches mentioned for the other three respirometers. For example, while the flow rates and $S_{O,in}$ must be measured, the coefficients $K_L a$ and S_O^* must be assessed from the dynamics of DO concentration.

Measuring oxygen in the gas phase

For this type of respirometers, both the gaseous and the liquid phases are involved. The biomass is contained in the liquid, while the oxygen measurements are performed in the gas phase. Concerning these oxygen measurements, they are obtained by measuring the change in the magnetic field caused by the presence of oxygen. The change recorded is proportional to the concentration of gaseous oxygen. It is possible to observe the analogy between the gas and the liquid phase respirometers. This group of respirometers encloses the following:

- Static gas – static liquid, GSS
- Flowing gas – static liquid, GFS
- Static gas – flowing liquid, GSF
- Flowing gas – flowing liquid, GFF

Table 14 summarizes the gas phase respirometers and their characteristics.

Table 14: Types of gas phase respirometers and main considerations

Static gas – static liquid, GSS	
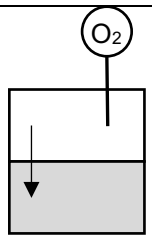 $\frac{d(S_O)}{dt} = K_L a(S_O^* - S_O) - r_O$ $\frac{d(V_G C_O)}{dt} = -V_L K_L a(S_O^* - S_O)$ (21)	This is the simplest gas phase technique for measuring r_O and includes the same DO mass balance to the liquid phase like LSS besides the one to the gas phase. Respiration rate r_O determination: $\frac{d(C_O)}{dt}$ must be measured and $\frac{d(S_O)}{dt}$ is required. Disadvantages: like in LSS, oxygen must be replenished to increase DO concentration.

Table 14: types of gas phase respirometers and main considerations (cont.)

Flowing gas – static liquid, GFS

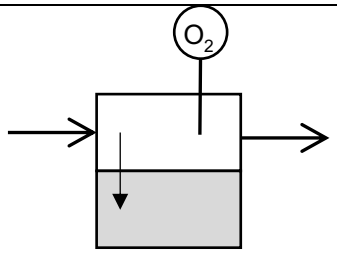

$$\frac{d(S_O)}{dt} = K_L a(S_O^* - S_O) - r_O$$

$$\frac{d(V_G C_O)}{dt} = F_{in} C_{O,in} - F_{out} C_O - V_L K_L a(S_O^* - S_O) \quad (22)$$

Continuous biomass aeration.

Respiration rate r_O determination: $\frac{d(C_O)}{dt}$ must be measured and $\frac{d(S_O)}{dt}$, F_{in}, F_{out}, $C_{O,in}$ and C_O are required.

Static gas – flowing liquid, GSF

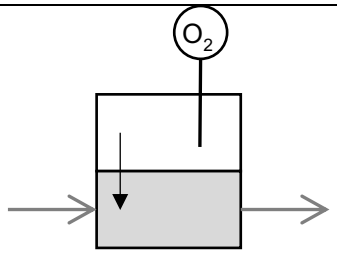

$$\frac{d(V_L S_O)}{dt} = Q_{in} S_{O,in} - Q_{out} S_O + V_L K_L a(S_O^* - S_O) - V_L r_O$$

$$\frac{d(V_G C_O)}{dt} = F_{in} C_{O,in} - F_{out} C_O - V_L K_L a(S_O^* - S_O) \quad (23)$$

The implementation of this technique cannot be found in the literature so far.

Flowing gas – flowing liquid, GFF

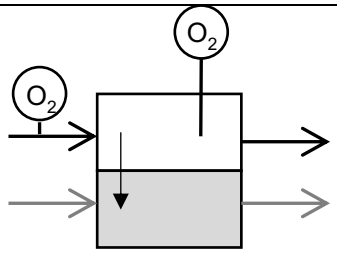

$$\frac{d(V_L S_O)}{dt} = Q_{in} S_{O,in} - Q_{out} S_O + V_L K_L a(S_O^* - S_O) - V_L r_O$$

$$\frac{d(V_G C_O)}{dt} = F_{in} C_{O,in} - F_{out} C_O - V_L K_L a(S_O^* - S_O) \quad (24)$$

Full mass balances, with no simplifications.

The GFF technique is the result of the application of the gas phase principle to a full-scale bioreactor. In general, combining L and G methods leads to more reliable respiration rate measurements.

Table 15 summarizes the eight types of respirometers, according to the processes involved in each setup.

Table 15: Processes involved in each type of respirometer

		LSS	LFS	LSF	LFF	GSS	GFS	GSF	GFF
Respiration	$V_L r_O$	-1	-1	-1	-1	-1	-1	-1	-1
DO accumulation	$\frac{d(V_L S_O)}{dt}$	-1	-1	-1	-1	-1	-1	-1	-1
Liquid flow	$Q_{in}S_{O,in} - Q_{out}S_{O,out}$			1	1			1	1
Interphase exchange	$V_L K_L a(S_O^* - S_O)$		1		1	1	1	1	1
Gaseous O accumulation	$\frac{d(V_G C_O)}{dt}$					-1	-1	-1	-1
Gas flow	$F_{in}C_{O,in} - F_{out}C_{O,out}$						1		1
Interphase exchange	$V_L K_L a(S_O^* - S_O)$					-1	-1	-1	-1

Oxygen Uptake Rate, OUR, measurements

The process of aerobic organic matter degradation described above is measured through the OUR, which provides an array of information about the performance of the treatment plant, the characteristics of the wastewater, and most importantly in this context, it provides information about the parameters needed for modelling (Hagman et al., 2007).

A respirometry test starts with the aeration of the system in order for all of the organic matter present to be consumed, before it reaches its endogenous level – the minimum oxygen consumption for the bacteria to maintain themselves. Once DO is at the saturation level, a rapidly consumed substrate (like acetate) is added to the system as a pulse. Aeration must be supplied in order to maintain a minimum level, 2 mg O_2/L, so that oxygen does not become a limiting factor (Ortigara, 2013). An example for DO behaviour in an LSF respirometer is given in Figure 4.

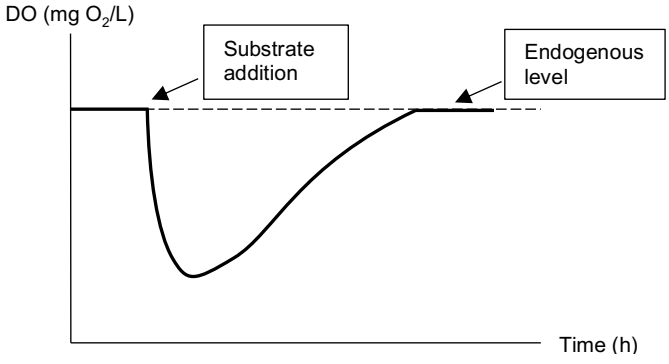

Figure 4: DO behaviour in an LSF respirometer after addition of acetate

OUR (mg O_2/(L·h)) values are obtained from equation 25, using a reactor's DO (mg O_2/L) values recorded over a certain time interval and hydraulic retention time (contact time the influent spends inside a reactor).

$$OUR = \frac{DO_{in} - DO_{out}}{HRT} \tag{25}$$

OUR values obtained in such manner allow for the sketch of an OUR profile (Figure 5), from which valuable information regarding organic matter degradability may be obtained. In a case where different types of COD are present, different *plateaus* will correspond to different rates of consumption and therefore different fractions of biodegradable COD may be identified. One of such *plateaus* may be due to nitrification.

Readily biodegradable COD by heterotrophs may be added as a reference substrate, such as acetate, which is highly used for this purpose. The quicker the substrate is consumed, the steeper the slope of the OUR. Once each consumption has reached the end, the OUR stabilizes into a *plateau*. The final relevant *plateau* corresponds to the level of endogenous respiration.

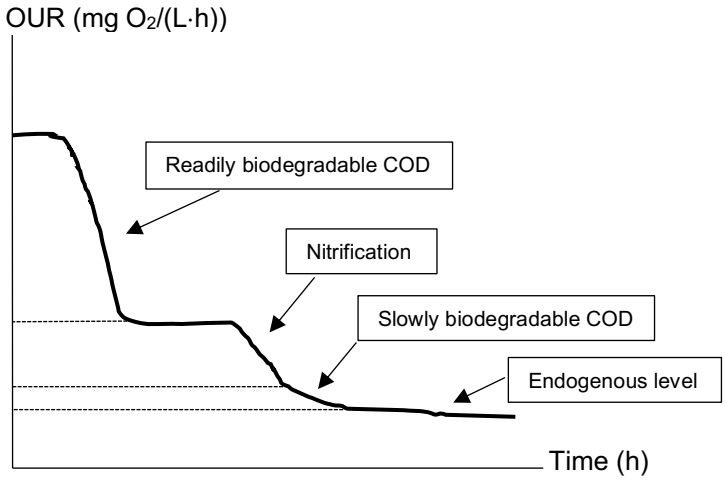

Figure 5: OUR profile and different rates of consumption, adapted from (Hagman, La, and Jansen 2007)

The quantification of the oxygen consumption for each type of COD biodegradability further supplies information for the determination of biokinetics such as maximum OUR for readily biodegradable COD – corresponding to the initial portion– and maximum OUR for nitrification – in turn referring to the second portion (Figure 6).

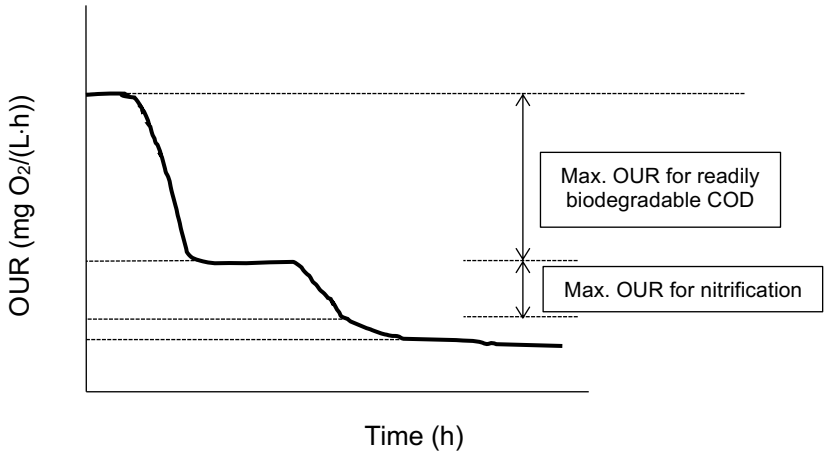

Figure 6: OUR profile with different rates of consumption and corresponding biokinetics

Storage mechanisms

The SSAG model's explanation for substrate allocation simultaneously for growth and storage allows for another important visual interpretation of the respirograms, which refers to the determination of stoichiometric parameters like growth yield, Y_H, and storage yield, YH_{STO}.

By adding a nitrification inhibitor, the OUR profile will no longer present the portion of oxygen consumption associated to nitrification and will instead present the following aspect (Figure 7):

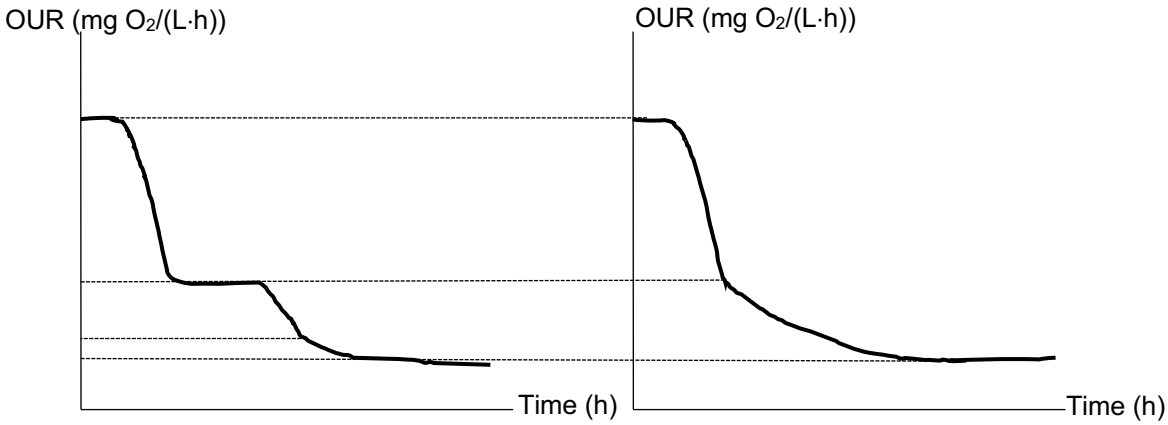

Figure 7: OUR profile with (left) and without (right) nitrification inhibitor

This in turn will allow for the definition of two more areas in the respirogram: the oxygen consumption dedicated to initial growth of heterotrophs and the oxygen consumption for growth on stored COD (Figure 8).

By recording DO values from the initial stage of the respirometric test, one obtains the endogenous level before the addition of the acetate substrate as well.

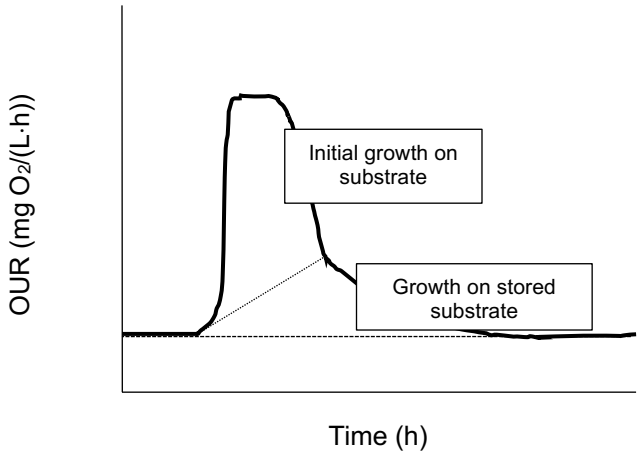

Figure 8: OUR profile of substrate and nitrification inhibitor addition where initial growth and growth on stored products are identifiable

2.5.3 Respirometry as an assessment tool for biokinetic and stoichiometric parameters

This technique has been widely used in the past for the characterization of wastewaters and biomass in activated sludge. Based on the models of ASM1, ASM2 and ASM3, several authors have applied respirometry for control of the AS process (Spanjers et al., 1996) for rapid characterization of wastewater and AS (Spanjers et al., 1995), and for determining kinetic and stoichiometric parameters in ASMs (Liwarska-bizukojc 2011), to name a few.

As far as the application of respirometry in TW, the works of Andreottola et al. (2007), Ortigara et al. (2011) and Pisoeiro et al. (2017) briefly presented next were dedicated to the assessment of biokinetic and stoichiometric parameters. Table 16 compiles the type of respirometer used in each case and the main parameters assessed.

Table 16: Parameter assessment by different authors with different types of respirometers

Author	TW/Type of respirometer	Parameters assessed
Andreottola et al. (2007)	VSSF/LSF	Endogenous respiration Max. rate of RBCOD oxidation Max. rate of nitrification
Ortigara et al. (2011)	VSSF/LSF	Endogenous respiration Max rate of RBCOD oxidation (with acetate) Max. OUR (with acetate) Max. OUR (with wastewater) Growth yield, Y_H Storage yield, Y_{STO}
Pisoeiro et al. (2017)	HSSF/LSS	Initial growth yield, Y_S Storage yield, Y_{STO}

Firstly, it must be indicated that the values of the parameters assessed in the studies in Table 16 are not comparable amongst them, given that different techniques, conditions and types of TW were studied. For this reason, they were not included. However, one can notice the need for further experimental data, which is the motivation behind the study developed for this thesis.

Moreover, because of the different terminology adopted by different authors, caution is necessary when comparing parameters, given that the approaches to modelling of the biological phenomenon and terminology may also differ.

What follows is a brief description of the three studies carried out so far, with the purpose of assessing biokinetic and stoichiometric parameters in order to provide with more data for the CWM1.

In addition, it was included the main results from the investigation carried out by Sin et al. (2005) for the modelling of SSAG processes in Activated Sludge, in order to provide further information relative to storage phenomena.

Respirometric techniques for assessment of biological kinetics in constructed wetland, Andreottola et al. (2007)

The first study dedicated to the use of respirometry in TW was developed by a research program between Italy and Brazil. In it, the authors intended to propose the application of an off-site respirometric procedure dedicated to the measurement of biokinetics in wetland soil cores. Specifically, the proposed technique aims to verify the ability of TW in performing organic matter oxidation and nitrification, as well as to measure their relative kinetic rates.

Two different types of respirometric tests were carried out: one with fresh wastewater and the other type with pure substrates.

A VSSF system was simulated at lab-scale with the construction of columns with different filling media, which were fed with fresh municipal pre-settled wastewater. Table 17 lists the main characteristics of the column. The characteristics of such water were measured, and the columns were left for a month in order to acclimate. During this period, the system was spontaneously aerated during sequential phases of fresh wastewater filling and discharge.

The respirometer was the column itself, with a DO probe at the top (inlet) and another one at the bottom (outlet), with data of DO concentrations being recorded every minute. An air pump assured aerobic conditions to the completely mixed column. Moreover, in order to maintain a constant temperature of 20ºC, the respirometer was kept in an incubator.

Typical of LSF respirometers, DO concentration is a limiting factor, and for this reason the system under analysis was provided with continuous forced aeration in order to allow the evaluation of the oxygen consumption for a longer time.

Table 17: Characteristics of TW sampled by (Andreottola et al., 2007)

Dimensions	h = 80 cm, ϕ = 12,5 cm
Volume of wastewater added	3,2 L
Filling media, from bottom to top	Total h = 60 cm, total V = 7,4 L. Gravel: h = 20 cm, particle size, ps: 30-70 mm, porosity, p = 33% Gravel: h = 10 cm, ps: 6-16 mm, p = 30% Sand: h = 20 cm, ps: 1-6 mm, p = 25% Sand: h = 10 cm, ps: 1-3 mm, p = 27%
Hydraulic retention time, HRT	0,2 h
COD load	55 gCOD $m^{-3}d^{-1}$
Type of respirometer	LSF

Respirometry of fresh wastewater

Respirometry test: these tests consisted of filling the colonizes VSSF column with fresh wastewater with the respective DO top and bottom continuous measurements. Besides the air pump, the system included another one for flow recirculation. The DO values were converted into OUR values according to Equation 26, in order for the respirogram to be produced. The hydraulic retention time, HRT of 0,2 h corresponded to the contact time between the water and the soil from the bottom to the top of the column. HRT is obtained from the ratio V_L/Q.

$$OUR = \frac{DO_{top} - DO_{bottom}}{HRT} [mgO_2 L^{-1} h^{-1}] \quad (26)$$

Stoichiometric and kinetic parameters calculated: Considering the integrals comprised between the respirogram and the endogenous respiration as the total amount of oxygen required for each event, ΔO_2, and considering the equivalence between ΔO_2 and ΔCOD, Equation 27 was then applied to calculate the yield coefficient, Y_H (mg_{COD}/mg_{COD}).

$$\Delta COD = \frac{\Delta O_2}{1 - Y_H} [mgCOD\ L^{-1}] \quad (27)$$

The main results obtained for these respirometric tests were the indicated in Table 18.

Table 18: Stoichiometric and kinetic parameters from respirometry of fresh wastewater calculated by Andreottola et al. (2007)

OUR after wastewater addition [$mgO_2\ L^{-1}\ h^{-1}$]	22
OUR from endogenous respiration [$mgO_2\ L^{-1}\ h^{-1}$]	6
ΔO_2 from oxidation of external substrates (total) [$mgO_2\ L^{-1}$]	190
ΔO_2 from readily biodegradable COD (RBCOD) [$mgO_2\ L^{-1}$]	14,6
ΔO_2 from nitrification [$mgN\ L^{-1}$]	96
Y_H [mg COD/mg COD]	0,67

Respirometry of pure substrates: acetate and ammonia

Respirometry test: The works of Andreottola et al. (2007) conducted one more type of respirometric tests in order to further confirm the kinetics present in VSSF columns, using pure substrates: acetate as RBCOD and ammonia as substrate for nitrification.

Main observations: as a result of the tests, Figure 9 presents the respirograms corresponding to the addition of acetate and ammonia. The evaluation of such profiles allowed for the calculation of the maximum rate of oxidation of RBCOD, maximum rate of nitrification and endogenous respiration, which can be found in Table 19. The endogenous values were firstly stabilized, and the addition of the pure substrates followed.

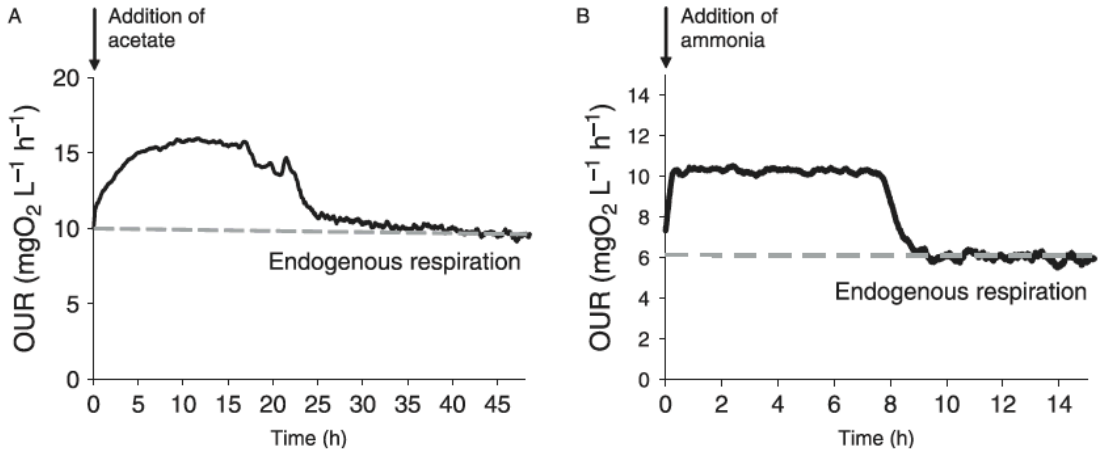

Figure 9: Pure substrate addition respirometry tests: a) acetate as RBCOD and b) ammonia as substrate for nitrification, Andreottola et al. (2007)

Main results: from the respirometry tests of pure substrate addition, the results in Table 19 were obtained.

Table 19: Stoichiometric and kinetic parameters from respirometry of pure substrates calculated by Andreottola et al. (2007)

Endogenous respiration [$mgO_2\ L^{-1}\ h^{-1}$]	6 – 10
Maximum rate of RBCOD oxidation [$mgO_2\ L^{-1}\ h^{-1}$]	5,8
Maximum rate of nitrification [$mgN\ L^{-1}\ h^{-1}$]	4,2

Main conclusions from Andreottola et al. (2007): As one of the pioneer studies in respirometric techniques applied to TW, particularly to VSSF TW with the use of an LSF respirometer, Andreottola et al. (2007) were able to visually identify in the respirograms the different phases corresponding to the endogenous level, the moment of S_S addition and its depletion, the nitrification phase up to the complete depletion of external substrates and the return of the OUR profile to the endogenous level. The identification of these processes allowed for the calculation of their single contributions of oxidation ΔO_2, which in turn permitted the calculation of the yield coefficient, Y_H. Moreover, by conducting respirometric

tests with pure substrates of acetate and ammonia, the authors were also able to calculate the maximum OUR for RBCOD and the maximum rate of nitrification.

Kinetics of heterotrophic biomass and storage mechanisms in wetland cores measured by respirometry, Ortigara et al. (2011)

In order to further explore the methodology proposed by Andreottola et al. (2007), in 2011 Ortigara et al. investigated a similar setup of columns representing VSSF TW, with slight differences (namely the particle size of the gravel used, the corresponding porosity and COD load) (Table 20). The same type of respirometer LSF was used, following the setup proposed by Andreottola.

Table 20: Characteristics of TW sampled by Ortigara et al. (2011)

Dimensions	ϕ = 12,5 cm
Volume of the respirometer	3,2 L
Filling media, from bottom to top	Total h = 60 cm, total V = 7,4 L. Gravel: h = 20 cm, particle size, ps: 15-30 mm, porosity, p = 31% Gravel: h = 10 cm, ps: 7-15 mm, p = 31% Sand: h = 20 cm, ps: 1-6 mm, p = 28% Sand: h = 10 cm, ps: 1-3 mm, p = 31%
HRT	0,18 h
COD load	40 gCOD $m^{-3}d^{-1}$
Type of respirometer	LSF

Similarly to the work that preceded this one, two types of respirometric tests were performed, one with wastewater and the other with a pure substrate of acetate. In the case of this work, storage mechanisms were also investigated in the respirometry with pure acetate. Allylthiourea was used in order to avoid nitrification in the cores and allow only oxygen consumption by heterotrophic bacteria. Another important novelty provided by this study was the following: in order to have a comparison term between respirometry of TW cores using wastewater and activated sludge, respirometric tests to activated sludge were also performed.

Respirometry of activated sludge

DO values were recorded from closed-respirometers, with aeration and mixing, in an environment with controlled temperature, to which 1,2 L of activated sludge taken from the oxidation tank of the WWTP in Trento Nord (Italy) were added intermittently. Before the addition of the activated sludge, the core was left to aerate overnight, to establish the endogenous level. DO concentrations were considered as being dependent on two factors: variations in room temperature, which cause variations in DO levels, and immediate significant decrease of DO concentrations with the addition of a substrate (acetate) spike addition.

In order to solve temperature variations, Equation 28 which represents a simplified form of the Arrhenius equation was used to correct OUR values to the reference temperature of 20ºC:

$$OUR_{20^{o}C}\frac{OUR_t}{\alpha(T-20^{o}C)}(\alpha=1.08) \quad (28)$$

Respirometry of pure substrate (acetate) and storage mechanisms

Respirometry test: addition of S_S – acetate – of 187 mgCOD/L to two different cores and correction to 20ºC.

Main observations: in both cores, four different phases can be observed in Figure 10, which are composed by

1) initial endogenous level, 4-5 $mgO_2\ L^{-1}h^{-1}$
2) rapid OUR increase from SS addition, OUR peak and rapid decrease after depletion
3) slow OUR decrease, in a generally non-linear fashion
4) endogenous level, 4-5 $mgO_2\ L^{-1}h^{-1}$

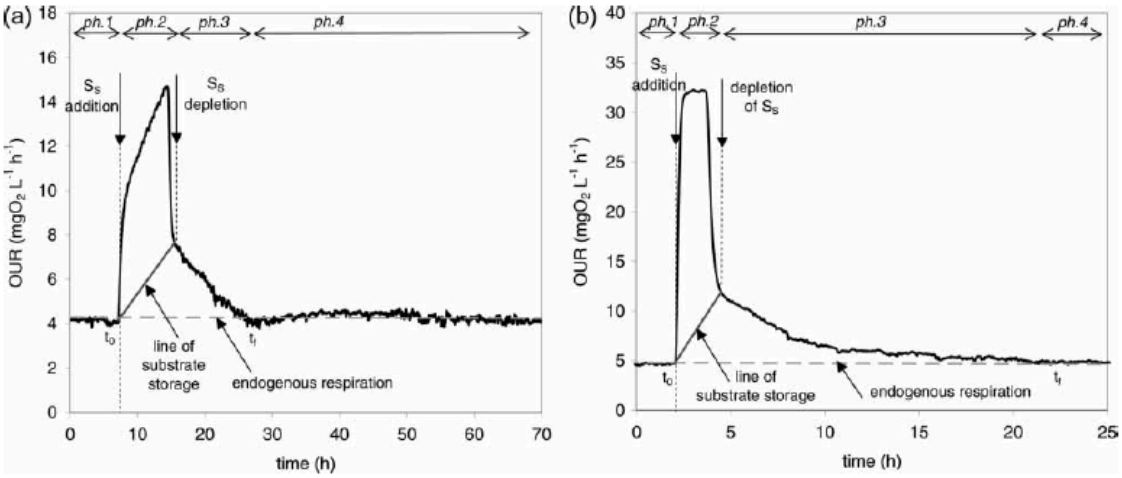

Figure 10: Pure substrate addition respirometry tests with acetate to TW cores a) and b), adapted from Ortigara et al. (2011)

The observation of S_S addition and its depletion allowed for the inference on the conditions for the biomass at that time: feast followed by famine. As explained by the SSAG model, in feast conditions there is simultaneous consumption of S_S (RBCOD) and gradual formation of internal storage products, X_{STO}. Once S_S depletion takes place, the biomass undergoes famine conditions, where its growth is due to the consumption of X_{STO}, represented by the mentioned slower OUR decrease before the endogenous level. According to the authors, the storage mechanism in TW cores is possibly a result of the intermittent loads which cause transient and highly dynamic load conditions, especially if longer feast/famine periods are applied.

Stoichiometric and kinetic parameters calculated: Maximum growth yield, Y_H (mg_{COD}/mg_{COD}) and growth yield on stored products, Y_{STO} (mg_{COD}/mg_{COD}).

Y_H (eq. 29) was calculated with the same relation used by Andreottola et al. (2007):

$$Y_H = 1 - \frac{\Delta O_2}{S_S} = 1 - \frac{\int_{t_0}^{t_f} [OUR(t) - OUR_{endogenous}(t)]dt}{S_S} \; [mgCOD/mgCOD] \quad (29)$$

The calculation of Y_{STO} was obtained through eq. 30:

$$Y_{STO} = 1 - \frac{\Delta O_{STO}}{S_S} \; [mgCOD/mgCOD] \quad (30)$$

Main results: Table 21 includes the main results obtained for respirometry with pure substrate. The values of maximum OUR and maximum COD removal do not include the endogenous respiration.

Table 21: Stoichiometric and kinetic parameters from respirometry of pure substrate calculated by Ortigara et al. (2011)

	Column (a)	**Column (b)**
Endogenous respiration [mgO_2 L^{-1} h^{-1}]	1,9	2,0
Maximum OUR with acetate [mgO_2 L^{-1} h^{-1}]	4,4	11,8
Maximum COD removal rate w/acetate [mgCOD L^{-1} h^{-1}]	5,0	26,8
Y_H [mg COD/mg COD]	0,59	0,56
Y_{STO} [mg COD/mg COD]	0,75	0,77

It is noteworthy that even though the kinetics for core b) were higher, their Y_H and Y_{STO} values were very similar. This has to do with the fact that the kinetics are dependent on the amount of biomass in the core, while stoichiometric parameters are independent of it.

Respirometry of TW core and activated sludge with municipal wastewater

Respirometry test: Municipal wastewater was added to both the activated sludge and the TW cores, once their endogenous levels were established.

Main observations: from the observation of Figure 11, one can note that

- the complete oxidation of the added wastewater takes a longer time in the TW core relatively to the AS (29,6 h versus 7,5 h);
- ΔO_2 from RBCOD oxidation is higher in AS (18,5 mgO_2 L^{-1} h^{-1}) than in TW core (11,6 mgO_2 L^{-1} h^{-1}).

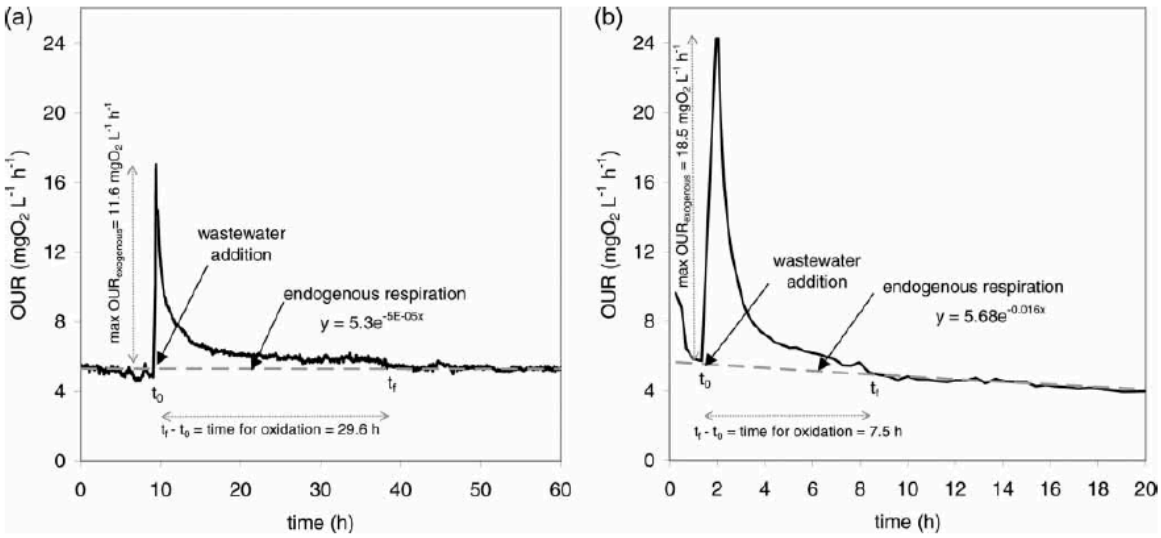

Figure 11: Respirograms of wastewater oxidation in TW core (left) and AS (right), Ortigara et al. (2011)

Stoichiometric and kinetic parameters calculated: Y_H for the TW core, BCOD and biomass decay rate.

According to the authors, the quantification of biodegradable COD (BCOD) was made possible with the procedures for AS proposed by Spanjers & Vanrolleghem (1995) and Vanrolleghem et al. (1999), adapted to the specific case of TW cores (eq. 31):

$$BCOD = \frac{1}{1 - Y_H} \times \frac{V_{ww} + V_L}{V_{ww}} \times \int_{t_0}^{t} \left[OUR(t) - OUR_{endogenous}(t)\right] dt \ \ [mgCOD/L] \tag{31}$$

V_L corresponded to the volume of liquid in the respirometer, 3,2 L, and V_{ww} to that of the added wastewater, 1,5 L. Note that the integral in equation 31 is the oxygen consumption previously described as ΔO_2.

Noting the endogenous lines depicted in Fig. 11, the equations of the line estimated for the TW core and the AS respectively are given by $y_{TWcore} = 5{,}3e^{-5\times10^{-5}x}$ and $y_{AS} = 5{,}68e^{-0{,}016x}$. These supply another kinetic parameter: the decay rate. The fact that the decay rate for the TW core is much slower than that of the AS suggests that the decay of biomass in TW cores is slow or of negligible variations within the relatively short period of 60h.

Main results: Table 22 gathers the main results relative to wastewater respirometry of a TW core and activated sludge.

Table 22: Stoichiometric and kinetic parameters from respirometry of wastewater of a TW core and activated sludge calculated by Ortigara et al. (2011)

	TW core	**Activated sludge**
Endogenous respiration equation	$y_{TWcore} = 5{,}3e^{-5\times10^{-5}x}$	$y_{AS} = 5{,}68e^{-0{,}016x}$
Biomass decay rate [1/d]	b = 5 x 10^{-5}	b = 0,016
Maximum rate of RBCOD oxidation [mgO_2 L^{-1} h^{-1}]	11,6	18,5
Y_H [mg COD/mg COD]	0,575	0,67 (assumed)
BCOD [mgCOD/L]	182	214

Main conclusions from Ortigara et al. (2011): Besides applying the knowledge developed in the previous study, Ortigara et al. (2011) explored the SSAG model to calculate the storage yield, Y_{STO}, in a VSSF TW with an LSF respirometer. In this study, the variations in DO readings due to temperature fluctuations were considered and were corrected with a form of the Arrhenius equation. For the determination of Y_{STO}, the use of a nitrification inhibitor was introduced to limit the tests to COD oxidation, without the interference of nitrification. The authors further concluded that, in comparison to activated sludge, the oxidation of wastewater in a TW core takes much longer to be completed, and its maximum OUR for RBCOD is lower. Furthermore, by estimating the endogenous level line equation, the authors were able to determine the biomass decay rate, which revealed itself close to zero for TW cores, and much lower than that of the activated sludge. This behaviour suggested that for TW cores the decay rate is slow or has negligible variations in a short period of 60h.

Determining stoichiometric parameters of detached biomass from a HSSF-CW using respirometry, Pisoeiro et al. (2017)

The novelty of this work was that it tested a horizontal sub-surface flow TW when the published work at the time had only approached vertical flow TW. Moreover, this study introduced the use of an LSS respirometer. An LSS respirometer was built where biomass from a HSSF-TW was tested. An easily replicable methodology was proposed, which involved the detachment of biofilm from the TW medium and the performance of tests with the obtained suspended biomass.

System setup: the setup of the system was composed of

- a cylindrical main reactor, made of acrylic, with a closed bottom and inlet-outlet ports;
- a turbine stirrer inside the reactor to promote fully mixed conditions;
- an air compressor connected to a perforated pipe at the bottom of the reactor to provide aeration to the biomass suspension;
- a custom-made glass respirometric cell with no aeration;
- a DO probe tightly attached to the cap of the respirometric cell, to prevent external aeration;
- a magnetic stirrer inside the cell to ensure homogeneous readings and to avoid biomass attachment to the probe and cell walls;
- a hydraulic pump to circulate the water between the reactor and the respirometric cell;
- a computer connected to the probe to record the DO readings.

Biomass source and sampling: the biomass used in the tests was sampled from a HSSF-TW (1,1 m x 0,71 m x 0,76 m), installed at the IST's Hydraulics Laboratory, with a filling media composed of 35 cm of gravel with a porosity of 30%. The water was kept 5 cm below the surface, which was planted with *Phragmites australis*. The HSSF-TW was fed with a synthetic sewage with a COD content of 800 mg/L, and feeding was done in batch-mode 5 days a week with a resting period during the weekends, at a rate of 10L/day. The sampling of the biomass was made from the extraction of 300 ml bulk volume of gravel and detached with a 2-min vigorous shaking with 1 L of tap water. Once most of the biomass was observed to be in suspension, the entire 1 L of water was separated from the gravel and immediately transferred into the reactor. A known volume of tap water was then added to a final volume of approximately 2,5 L.

Respirometry test: 100 mL of a sodium acetate solution, S_S, were added (COD levels in the reactor between 50 and 100 mg/L) once the endogenous level was stabilized. The OUR values were obtained from the slope of the linear regression line of DO data points along time in idle periods. A nitrification inhibitor was used as well, in order to prevent any nitrification during the tests.

Main observations: after performing a total of 10 respirometry tests with addition of pure substrate the authors were able to identify three types of OUR profiles, presented in Figure 12, which revealed how variable the biomass behaviour can be. The three types of profiles showed evidence of storage and allowed for the identification of the period of RBCOD consumption, which was performed visually, according to the methodology proposed by the two previous studies mentioned, by Andreottola et al. (2007) Ortigara et al. (2011).

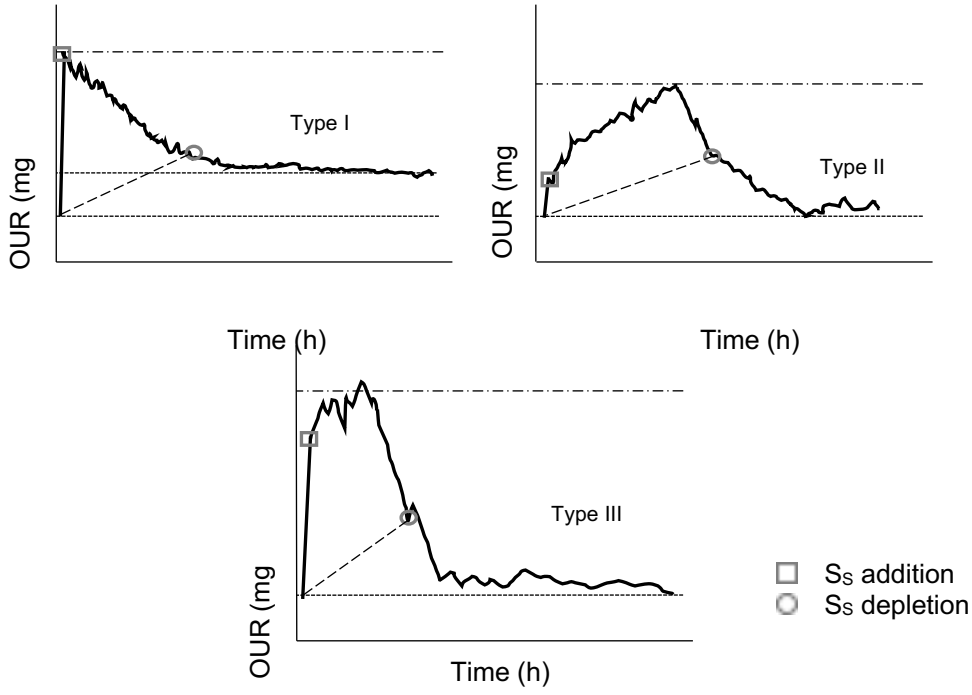

Figure 12: Three types of respirograms, adapted from Pisoeiro et al. (2017)

In type I profiles, the peak resultant from maximum OUR due to the oxidation of the external substrate happens immediately after S_S addition and is similar to the one obtained by Ortigara et al. (2011). OUR then decreases to a value close to the endogenous level, but before stabilizing, two different slopes are identifiable: a steeper one associated to the consumption of the external substrate, and a slower decrease related to the consumption of the stored products. The example provided for type I profiles ends in a level higher than that of the initial endogenous, which can be attributed to the biomass attachment to the walls of the cell, or to it might mean that the test was not complete and storage products were still being consumed.

Type II profiles were characterized by starting at a lower OUR value after S_S addition. A steady increase then follows, until maximum OUR is reached. The profile then drops in a steeper slope and after the consumption of S_S, the OUR profile continues to decrease but in a slower manner (consumption of X_{STO}), until the initial endogenous level is again reached.

After the S_S addition in type III profiles, the OUR line increases and maintains itself in a plateau of high values, until all of the acetate is consumed. The profile then drops until a level higher than that of the endogenous respiration, and the consumption of the stored products takes place until their depletion, which corresponds to the profile reaching again the endogenous level.

Stoichiometric and kinetic parameters calculated: initial growth yield, Y_S, and storage yield, Y_{STO}. The initial growth yield was obtained from the Equation 32, which is similar to that of the overall growth yield, Y_H, used by Andreottola et al. (2007), but includes the subtraction of the storage oxygen consumption integral:

$$Y_S = 1 - \frac{\Delta O_{2_{acetate}}}{S_S} = 1 - \frac{\int_{t_0}^{t_f}\left[OUR(t) - OUR_{endogenous}(t) - OUR_{STO}(t)\right]dt}{S_S}\ [mgCOD/mgCOD] \quad (32)$$

The calculation of Y_{STO} was done considering the oxygen consumption during the use of the storage components, at the end of the respirograms. This approach follows that of several studies in AS, such as Carucci et al. (2001).

Main results: the values of the respirometry tests resulting in the three different types of profiles are presented in Table 23.

Table 23: Stoichiometric and kinetic parameters from respirometry of pure substrate calculated by Pisoeiro et al. (2017)

Type of profile	No. of tests	S_S range [mgCOD/L]	Y_S [mg COD/mg COD]		Y_{STO} [mg COD/mg COD]	
			range	average	range	average
I	5	42-100	0,56-0,77	0,67	0,78-0,87	0,83
II	3	47-133	0,34-0,51	0,41	0,65-0,83	0,75
III	2	47-64	0,46-0,49	0,48	-	0,83

Main conclusions from Pisoeiro et al. (2017): As the novelty of this study was the application of respirometry in HSSF TW and the use of an LSS repirometer, the authors proposed a setup with detached biomass from the TW, allowing for respirometric testing *ex situ*. This study adapted the procedures of Ortigara et al. (2011) with the use of the nitrification inhibitor and the temperature corrections and introduced the calculation of another stoichiometric parameter: the initial growth yield, Y_S. With a higher number of tests performed, Pisoeiro et al. (2017) were able to identify a pattern and classify three different types of OUR profiles, which indicated how variable the biomass behaviour can be.

A new approach for modelling simultaneous storage and growth processes for activated sludge systems under aerobic conditions, Sin et al. (2005)

In order to allow for better modeling concerning simultaneous storage and growth processes (the first phenomenon initially explored in ASM3), the authors of this work took on the task of developing a new model and pair it with the use of an optimal experimental design (OED) procedure that would increase its robustness.

Although the research of Sin et al. (2005) was relative to the respirometric testing of biomass sampled from activated sludge of full-scale operating WWTPs and not TWs, it was considered relevant to have their findings of stoichiometric parameters and kinetics as a comparison term to the work developed for this thesis. What follows is a brief explanation of the developed SSAG model, the procedures of this work and its main findings.

Main research goals: the main goals of this work can be divided into two, which are given by (1) the development of a new model (the SSAG model) accompanied by a calibration methodology based solely on batch OUR data, and a practical identifiability analysis of the model parameters, and (2) the use of an optimal experimental design (OED) tool that could improve the parameter estimation accuracy using OUR measurements alone. Better insight on these steps is given below but only the matters relative to the estimation of the parameters of interest in the context of this thesis – Y_H, Y_{HSTO} and Y_{STO} – will be highlighted in the next lines.

Theoretical procedures for parameter estimation: both procedures (1) and (2) were used to perform respirometry tests to biomass samples from activated sludge of full-scale operating WWTP and the results obtained from both methods were discussed by the authors.

(1) The development of the new SSAG model was accomplished by critically evaluating previously proposed models for feast/famine conditions and by developing a second order type kinetics expression to describe the degradation of stored products in the famine phase.

The SSAG model proposed by the authors comprised of kinetics for both the feast and the famine conditions. In particular, relatively to the feast phase, this model would significantly simplify the calculations of the growth yield on substrate ($mg_{COD\text{-}X}$/ $mg_{COD\text{-}S}$) represented by Y_H, of Y_{STO} the storage yield on substrate ($mg_{COD\text{-}STO}/mg_{COD\text{-}S}$) and $Y_{H,STO}$ the growth yield on storage products ($mg_{COD\text{-}X}/mg_{COD\text{-}}$

$_{STO}$). According to the metabolic model by van Aalst-van Leeuwen et al. (1997) for pure cultures (Beun et al., 2000, 2002; van Loosdrecht and Heijnen, 2002), the parameters Y_H, Y_{HSTO} and Y_{STO} are linked by the metabolism of the substrate and are dependent on the efficiency of oxidative phosphorylation (the efficiency of ATP generation in cells), given by δ. This fact restricts then the calculation of the three parameters to the determination of only δ (eq. 33 to 35).

$$Y_{H,S} = \frac{4\delta - 2}{4.2\delta + 4.32} \times \frac{4.2}{4} \tag{33}$$

$$Y_{STO} = \frac{4\delta - 2}{4.5\delta} \times \frac{4.5}{4} \tag{34}$$

$$Y_{H,STO} = \frac{4.5\delta - 0.5}{4.2\delta + 4.32} \times \frac{4.2}{4.5} \tag{35}$$

(2) A general scheme for the OED tool used in the research under consideration can be found in Figure 13, where an algorithm is intended to perform simulated experiments in order to quantify the potential effect of the proposed experimental conditions on the objective function. Its objective is to optimize experimental conditions relative to the objective function, and it requires a preliminary model capable of being identified in the basis of previously acquired data.

Biomass sampling and system setup: two sets of samples from AS were tested, (A) was extracted from a WWTP in Belgium and was tested in a hybrid-respirometer described in (Sin et al. 2005), while (B) was sampled from a WWTP in Spain and tested in an LSF respirometer.

Respirometry test: in both experiments (A) and (B), the systems were left to aerate overnight in order to reach the endogenous state, after which a first pulse of acetate was added to “wake up” biomass activity. Besides the acetate, ammonia and allylthiourea (ATU) were added to prevent growth limitation and nitrification, respectively. The respirometric tests then were performed by pulse addition of acetate accompanied by titrimetric measurements to allow indirect monitoring of S_S uptake from the medium (quality check of the respirometric measurements).

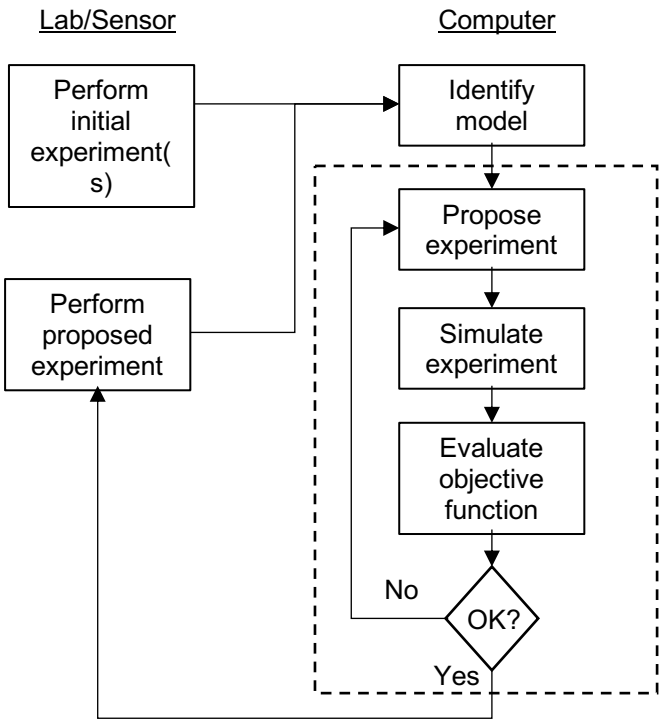

Figure 13: General procedure for experiment design, adapted from Dynamical Modelling and Estimation in Wastewater Treatment Processes, 2001

Main results: the OUR readings were then interpreted with the proposed SSAG model and with the OED tool developed for that research.

Although not presented here, the authors found that the results for the estimated parameters were better when the OED was used, but found there was no significant difference of approaches for the calculated parameters of Y_H, Y_{HSTO} and Y_{STO} given that the δ obtained from both approaches was very similar (Table 24).

Table 24: Stoichiometric parameters estimated by Sin et al. (2005) with SSAG model and OED tool

	SSAG proposed model		**OED tool**
	Experiment (A)	**Experiment (B)**	**Experiment (B)**
δ	2,56		2,88
Y_H [mg_{COD-X}/mg_{COD-S}]	0,61	0,58	0,57
Y_{HSTO} [$mg_{COD-STO}/mg_{COD-S}$]	0,71	0,68	0,68
Y_{STO} [$mg_{COD-X}/mg_{COD-STO}$]	0,83	0,81	0,80

Main conclusions from Sin et al. (2005): given that this work was relative to modelling in WWTPs instead of TWs, the two most relevant conclusions to be drawn in this context were that the yield coefficient for heterotrophic growth on acetate (around 0,58 mgCOD/mgCOD) resulted in a value lower than that of the reported value in the ASMs, and that the yield coefficient values for both experiments (A) and (B) were very similar even if they had such different growth and storage kinetics (which were

not presented here). Concerning the first conclusion mentioned, the authors believe this was due to the fact that the proposed SSAG model provides a better prediction of the growth yield in full-scale WWTPs given that it takes into consideration the storage phenomena. Regarding the second conclusion, it supports the validity of the model proposed, in which it is assumed that the macroscopic yield coefficients are independent of the growth rate and can be estimated using a metabolic relation.

3. Fixed biomass respirometry for determination of biokinetic and stoichiometric parameters in treatment wetlands

In order to supply new specific data to the current models used to describe kinetic processes in SSF TW – Constructed Wetland Model No1, Langergraber et al. (2009) – a new adaptation of an LSF (liquid phase principle – static gas and fluid liquid) respirometer was developed for fixed biomass testing in a HSSF TW. By directly extracting and analyzing the biomass attached to the gravel medium, it was intended to maintain its conditions in the TW as much as possible, which in principle would avoid problems identified in the detached biomass procedure used by Pisoeiro et al. (2017). On the other hand, similarly to the work of Pisoeiro et al. (2017), the adopted procedures permit the *ex situ* analysis of a working HSSF TW.

Until present date, with the exception of Pisoeiro et al. (2017), the works carried out to the date of this one referred only to vertical flow TWs and to the use of LSF respirometers (Andreottola et al. (2007) and Ortigara et al. (2011)).

Between March and August of 2018, a series of respirometry tests with sodium acetate trihydrate solution substrate were carried out at the Environmental Laboratory of IST. For that, a respirometer system was assembled with the use of everyday lab materials and new sets of biomass were sampled from a HSSF lab scale TW located inside the lab (none of the sampled beds were planted). The DO readings and consequent calculation of OUR profiles allowed for the determination of the yield coefficient for heterotrophic bacteria, Y_H, as well as the associated yield storage coefficient for heterotrophic bacteria, Y_{HSTO}. Furthermore, the profiles obtained from the tests were classified according to the type of profile (I, II and III) proposed by Pisoeiro et al. (2017).

3.1 Characteristics of the lab scale HSSF TW sampled

The TW lab scale installation from which the fixed-biomass sample was extracted was setup in 2012 by Galvão and Matos (2012) for the study of HSSF TW response to sudden organic load changes. The installation was composed of 9 PVC beds (B), 3 of which were continuously used in this present work – B2, B3 and B6.

In general terms, what distinguishes the beds amongst themselves is the concentration of the synthetic sewage which was used to feed them. Table 25 summarizes the general characteristics of the beds.

Table 25: Characteristics of HSSF TW sampled

Dimensions of the plastic beds	1.1 m × 0.71 m × 0.76 m
Filling media: gravel	h = 30 cm, particle size, ps: 4-8 mm, porosity, p = 30%
Average water level below surface	5 cm

The beds that were fed with a higher synthetic sewage concentration are B2 and B3, whilst B6 was fed with a lower concentration. Table 26 presents particular characteristics of these beds.

Table 26: Concentration of sampled beds (B)

	Synthetic sewage concentration (COD)	Feeding rate
B2	1600 mgO_2/L	
B3	1600 mgO_2/L	10 L/d, 5 days/week
B6	800 mgO_2/L	

The synthetic sewage used to feed the beds at a rate of 10 L/d, for 5 days a week with a resting period during the weekends was prepared with the components and quantities listed in Table 27. Two synthetic sewages were used with different CODs: the one of lower concentration of approximately 800 mg/L and one with a concentration two times higher, 1600 mg/L. The feeding of the beds was made through the dilution of the synthetic sewage solutions with tap water to complete 10L, placed in a reservoir for each bed, which was placed at a higher elevation, so that the solution would flow gravitically. COD tests were performed almost weekly to the influent and effluent of each bed.

Table 27: Composition of synthetic sewage solutions of 800 and 1600 mgO_2/L CQO

Components	800 mgO_2/L[a]	1600 mgO_2/L[b]
Urea (g)	30	36
Na-acetate $3H_2O$ (g)	132	355
Peptone (g)	17	47
Starch (g)	150	405
Powdered milk (g)	150	405
Soy oil (g)	15	17
Liquid gardening substrate (mL)	250	300

[a] added to create 5L of concentrate solution

[b] added to create 6L of concentrate solution

3.2 Description of the LSF respirometry system assembled

The system (Figure 14) was setup with conventional laboratory materials and was composed of a cylindrical PVC water tank, a plastic rectangular reactor closed with a plastic lid, a crystal pipe system for the water flow and two DO probes. The pipe system contained two plastic taps in the stretch between the pump and the rector: the first one as a water emergency exit, in case there were any clogging problems, and a second one for pulse acetate addition.

DO readings were performed at the inlet and outlet of the reactor, inside the water tank and immediately after the reactor, respectively. The DO inlet probe was placed in the water tank with a metal protection and the outlet probe was tightly enclosed in a glass cell supported by a claw, at the exit of the reactor. Also before the exit glass cell, a spongy filter was placed in the beginning of the exit pipe to prevent the dislodged biomass to enter the DO_{out} cell and cause false readings. The water tank contained a perforated pipe in the bottom connected to an air compressor to ensure oxygen levels close to saturation. A peristaltic pump allowed the water to circulate from the water tank through the system.

Table 28 discriminates the components of the system. The measurements were done to the liquid phase of the respirometer, the gas phase was stationary and its liquid phase flowing.

Table 28: Components of the LSF respirometric system

Peristaltic pump	FWT VPER-N
Air compressor	Hailea V-20
DO sensors	YSI ProODO (optical measurements)

The DO sensors performed readings at different rates: DO_{in} values were recorded every 20 seconds and stored in the probe's memory, while DO_{out} values were registered and stored every second in a computer.

While running, the system would always be covered with a blackout curtain fabric to protect it from light exposure (which interferes with the probes' optical sensors readings), and to prevent contamination from external sources.

1 – water tank

2 – DO_{in} probe

3 – perforated pipe

4 – air compressor

5 – persitaltic pump

6 – tap for flow control

7 – tap for S_S addition

8 – reactor

9 – DO_{out} probe

10 – glass cell

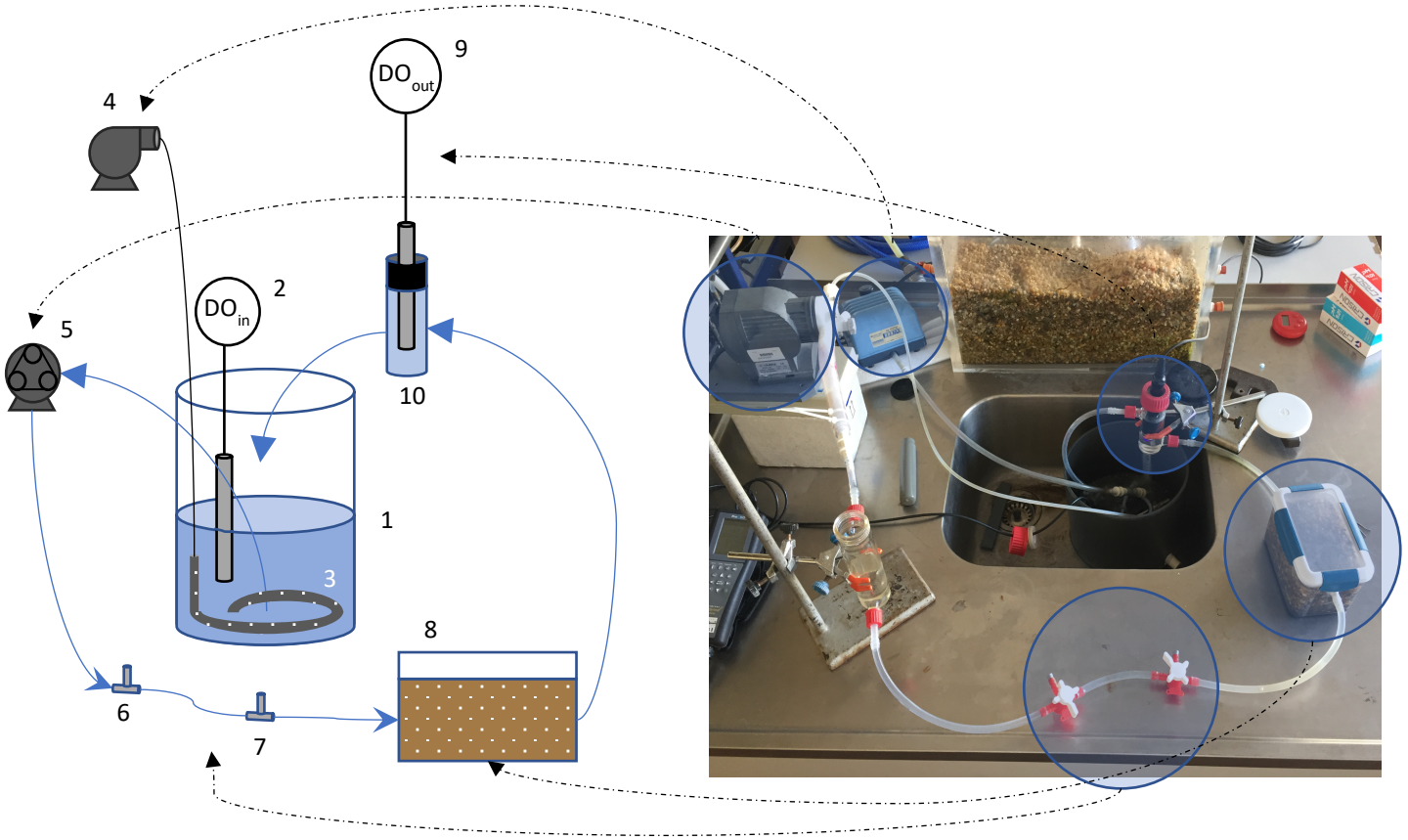

Figure 14: LSF respirometer setup scheme and correspondence with lab setup

3.2.1 Tracer tests for characterization of hydraulic properties

In order to assure a correct design of the TW, its hydraulic properties can be measured with the use of tracer tests. These allow for the assessment of parameters which allow inferring on the treatment efficiency of a given TW. In particular, treatment efficiency depends on the kinetics of the reactions (rate) and on the residence time. In an ideal reactor, all fluids experience the same residence time, in a plug-flow manner. In reality, there is a distribution of the residence time, which is due to different elements having different detention times, either longer (stagnant flow) or shorter (short circuiting). The wider the distribution of the residence time, the lower the efficiency of the TW. A tracer is injected in the system and the deviation of its behaviour when compared to a plug-flow is translated into a distribution of residence time, DRT. The DRTs are defined with numerical parameters, such as the mean residence time, $\bar{t}_m$, and the variance, σ^2, which in turn are obtained through a concentration versus time (C vs. t) curve. The tracer used should not alter the system's existing flow and should be nonreactive and nonsorptive (conservative). Its density must be similar to that of the system's fluid and evenly distributed along the fluid (Stairs 1993).

For the particular case of this study, the characteristics of the reactor used were assessed with a saline (NaCl) tracer – 16g – dissolved in 40L of tap water and added continuously to the system. Prior to the test a conductivity vs saline concentration curve was established by preparing solutions with increasing salt concentrations and measuring their conductivity.

The conductivity of the solution added for the tracer test was measured at 817 μS/cm and once this value was obtained at the outlet, the test had ended. Since the complete achievement of the inflow value is very unlikely, the criteria used to define the end of the test was when a vale of 813 μS/cm was achieved. The concentration (mg/L) versus time (minutes)is plotted in Figure 15.

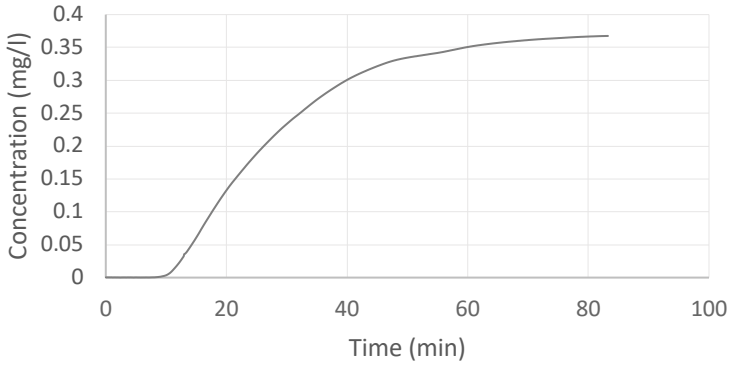

Figure 15: C(t) curve obtained for the tracer test

In order to calculate the mean residence time and the variance, a step-change integral modelling methodology proposed by (Bonner et al., 2017) was followed and the C(t) curve was transformed into a cumulative distribution curve, F(t), with Eq. 36 (Figure 16).

$$F(t) = \frac{C(t)}{C_{max}} \tag{36}$$

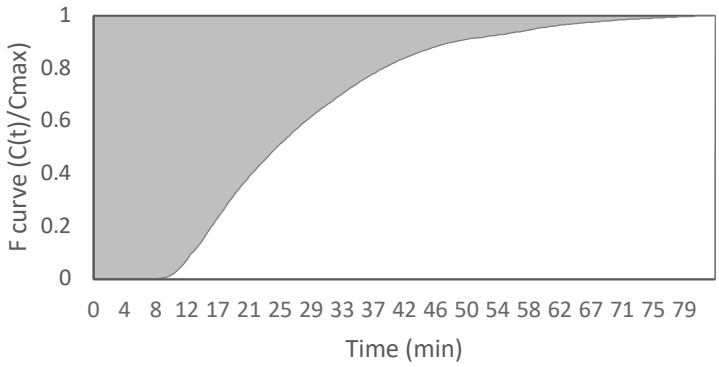

Figure 16: F(t) curve obtained from the C(t) curve

From the F(t) curve, the mean residence time and the variance were calculated with Eqs. 37 and 38.

$$\bar{t}_m = \int_0^\infty [1 - F(t)]dt \quad (37)$$

$$\sigma^2 = 2\int_0^\infty t[1 - F(t)]dt - \bar{t}_m^2 \quad (38)$$

Finally, the results obtained from the tracer test performed on the 30th of April to the reactor of the assembled LSF system were as summarized in Table 29. The mean residence time obtained at 28,27 min was close to the theoretical HRT $(\text{water volume in the system (mL)}/\text{water flow (mL/min)})$ used in the calculations throughout this work.

Table 29: Mean residence time and variation calculated with tracer test

Time (min)	28,27
σ^2 (min^2)	209,72
σ (min)	14,48
HRT_t	35

3.3 Respirometry tests with addition of pure substrate S_S of sodium acetate trihydrate

In general terms, each set of respirometry tests were conducted in the following manner:

Phase I – preparation of the system and establishment of the endogenous conditions

Phase II – set of respirometry tests with addition of a sodium acetate trihydrate solution

Phase III – determination of the sampled gravel's total and volatile solid contents

The solution of S_S is prepared with approximately 1 g of sodium acetate and 150 mL of distilled water. Two solutions were prepared during the experimental period: the first one prepared was used until the 28th of June and its COD was of 933,4 mgO_2/L, while the second solution prepared was used until the 12th of July and had a COD of 961,4 mgO_2/L.

For each set of tests, a approximate volume of 1400 cm^3 gravel media with the biomass in the form of a biofilm was extracted from a depth of approximately 10-15 cm of the bed (Fig. 15). A small volume of water was carefully passed through the sample to assure no remaining substrate was present. The gravel was then transferred into the reactor and the system was filled with a total of 3L of tap water. DO recordings were then started once the flow at the outlet stabilized at around 16 mL/min. The system was left circulating until the DO_{out} recordings exhibited an endogenous level (1 to 2 days). Once this level was attained, a volume of 1 to 9 mL of the sodium acetate solution was added. The DO probes were left recording until the end of the test, indicated by the level of DO_{out} reaching again the endogenous level. Once the S_S solution was introduced there would be a steep decrease in the DO line, indicating the uptake of the DO from the water for substrate consumption.

There were two phases to each set of tests: preparing the system and allowing endogenous conditions to stabilize and the respirometry itself. The steps of each phase are described in the next sections.

3.3.1 Phase I – Preparing the system for a respirometry test

The setup and preparation of the system before a respirometry test contemplated the following steps:

1. Extraction of biomass sample from the bed (Fig. 17) – a gravel sample (approximately 1400 cm^3) was extracted from the bed with a plastic container, from a relatively superficial depth (10-15 cm) from the point where the gravel started exhibiting a black coating indicating the presence of biofilm.
2. Light sample wash – with a metal strainer of a fine mesh (approximately 1 mm), the sample was placed under a small trickle of tap water in order to remove precipitates and residual substrate from previous feedings. This step was carried out with care to wash interstitial liquid while avoiding removing too much biomass.
3. Placement of the biomass in the system – the plastic reactor was then filled with the prepared sample leaving the last 2 cm from the top empty.
4. Addition of water to the system – 3L of tap water were then added to the water tank.
5. Starting the system – the air compressor and the pump were turned on to ensure full aerated conditions and as optimize flow rate through the pipe system, into the reactor and exiting to the water tank. The DO probes were set to start recording data in order to register the establishment of the endogenous level (identified on the computer to which the DO_{out} probe data was being recorder) and indicate when the respirometry test could be initiated.

About the water level in the reactor: once the water started flowing through the system, it was necessary to make sure its level inside the reactor was enough that it would almost submerge the gravel (approximately 2 cm from the top) without allowing it to assume a free flow manner. The water height was manipulated through flow control (on the pump) and the reactor's lid: with the reactor open, once the water filled up until the mark of the 2 cm from the top, the lid was placed closing the reactor and entrapping a top layer of air confining the desired volume of water.

About the outlet water flow: a constant flow – 10 to 20 mL/min – of water exiting the system and re-entering the tank was aimed at, by regular flow check. If the flow was too low, the system would be interrupted and the filter at the exit tube would be removed and washed. It should be noted that the amount of biofilm that was sometimes accumulated and washed from the filter was neglectable and did not influence the quantity of biomass in the system. Furthermore, this clogging problem was not encountered many times during this work. In case the flow was too high, the pump would be regulated.

About the eventuality of the system clogging: in case there was any perturbances which could cause the water to overflow, a security plastic tap with an open top was installed in the initial pipe stretch, from where the water could escape and be collected by a backup reservoir connected to the tank in order to return the water to the system (see Figure 18).

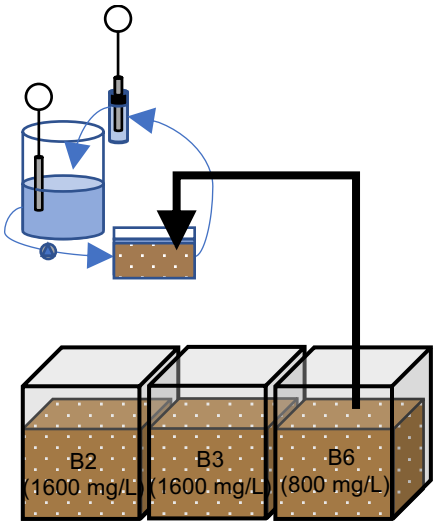

Figure 17: Bed sampling into the respirometer

3.3.2 Phase II – Respirometry test with acetate solution addition

1. Flow check – before the injection, the water volume at the exit was collected in a measuring cylinder for 1 minute, in order to determine if the flow (mL/min) remained constant.
2. Acetate addition – the solution was added by pulse injection at the second plastic tap in the initial pipe stretch that connected the water from the tank to the reactor (Figure 18). The pump was interrupted and an injection of 1 to 9 mL of the acetate solution was introduced in the system.
3. The pump was then restarted for the water to return to its circulation.
4. Test ending – by accompanying the DO_{out} recordings in the computer, once the DO line had returned to the endogenous level, the test was given as finished and the inlet and outle probes' recordings exported to the computer to be processed.

About inlet and outlet DO data processing: to obtain the OUR profiles relative to each test, an excel file with Visual Basics for Applications (VBA) routines was used to input DO readings.

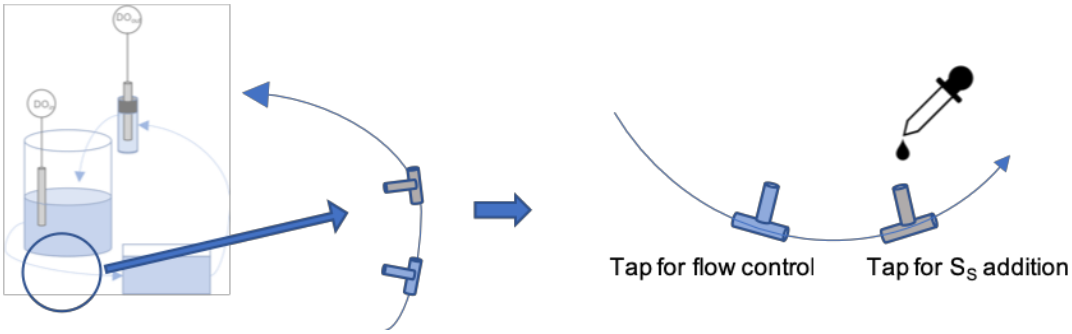

Figure 18: Pipe stretch with taps for flow control and S_S addition

3.3.3 Phase III – Determination of the sampled gravel's total and volatile solids

Each set of tests was concluded with the determination of the total solids (TS) and the volatile solids (VS) to allow assessing the amount of biomass in each round, according to Method 1683 by EPA (EPA, 2001).

Samples preparation – six gravel samples from the reactor were collected in metal evaporating discs with a perforated lid.

1. TS determination:
   - the samples were dried at 105ºC in a drying oven overnight, left to cool down to room temperature in a desiccator with silica and weighted;
   - they were placed in the drying oven again for another hour; if there was a difference in weight of 5%, they would be placed to dry for another hour, or until there were no more changes to their weight. The measured weights were registered as "W_{total}".

2. VS determination:
   - the now dried samples were placed in a muffle furnace for 2 hours at 505ºC, left to cool down to room temperature in a desiccator with silica and weighted;
   - they were placed in the muffle furnace for another hour or until there were no more changes of 5% to their weight. These final measured weights were registered as "$W_{volatile}$".

3. Calculation of total solids (TS), fixed solids (FS) and volatile solids (VS).

"W_{gravel}" is the difference between W_{zero} and the weight of the sampling disc, which was of approximately 2 g. The zero weight was obtained after the volatile fraction was left soaking in bleach over one or two night and after rinsing it with water; it was then placed again in the muffle furnace for 2 hours. The final measured weights were registered as "W_{zero}".

Equations 39, 40 and 41 were used as follows:

$$TS/gravel = \frac{W_{total} - W_{zero}}{W_{gravel}} \times 100 \quad (39)$$

$$FS/gravel = \frac{W_{volatile} - W_{zero}}{W_{gravel}} \times 100 \quad (40)$$

$$VS/gravel = \frac{W_{total} - W_{volatile}}{W_{gravel}} \times 100 \quad (41)$$

W_{total} = weight after 105ºC (g), W_{zero} = weight after bleach and 105ºC (g), $W_{volatile}$ = weight after 505ºC (g), W_{gravel} = $W_{zero} - 2$.

4. Determining biokinetic and stoichiometric parameters in a HSSF TW with an LSF respirometer

4.1 From DO readings to OUR profiles

In order to obtain the OUR profiles for each test, an Excel template with Visual Basics for Applications (VBA) programmed was used, where the DO inlet and outlet readings were inserted, along with other necessary variables, such as the volume of S_S (mL), the CQO of S_S (mg/L), and the porosity of the sampled gravel (30%). The profiles were also corrected to the standard temperature of 20ºC.

The OUR profiles and their corresponding temperature correction obtained were as the example presented in Figure 19:

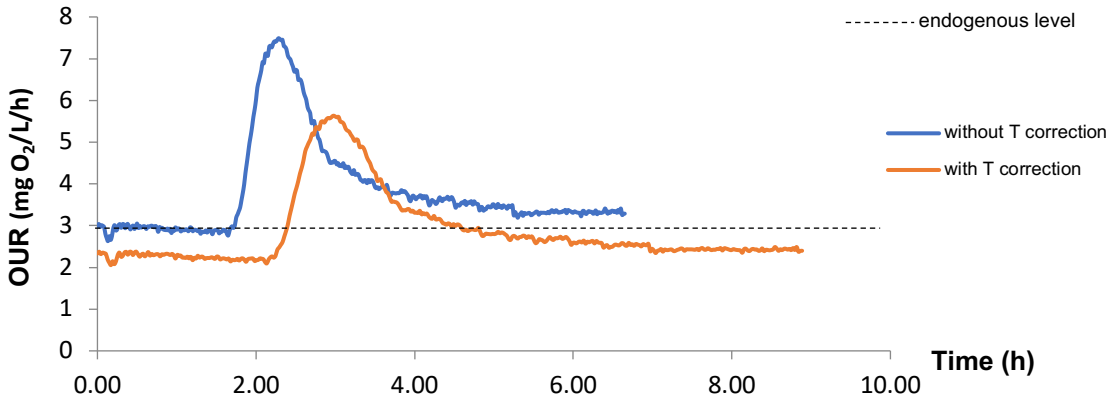

Figure 19: OUR profile of a respirometry test with acetate addition

Once the profiles were obtained, by visually identifying the key points of the test (Figure 20), a series of calculations were performed for the attainment of the desired parameters.

Respirometry with pure substrate results in one of two outcomes: a situation where there are no storage phenomena and one where these mechanisms take place. In case there is no storage, the oxygen consumption recorded by the probes (OUR profile) will only be due to the oxidation of substrate for growth of heterotrophic biomass. And so, the heterotrophic growth yield Y_H (mg_{COD}/mg_{COD}) is calculated with the integral (the area) comprised between the OUR line and the endogenous level. In a situation where storage is visually identified in the respirogram, a line is drawn from the point identified in Fig. 20 as “acetate depletion” to the point indicated as “begginig of the test”. It is assumed that the consumption of stored products is linear for as long as there is acetate in the system. In this scenario, the heterotrophic growth yield Y_H is attributed to the simultaneous growth of heterotrophic biomass and the production of storage products by these bacteria.

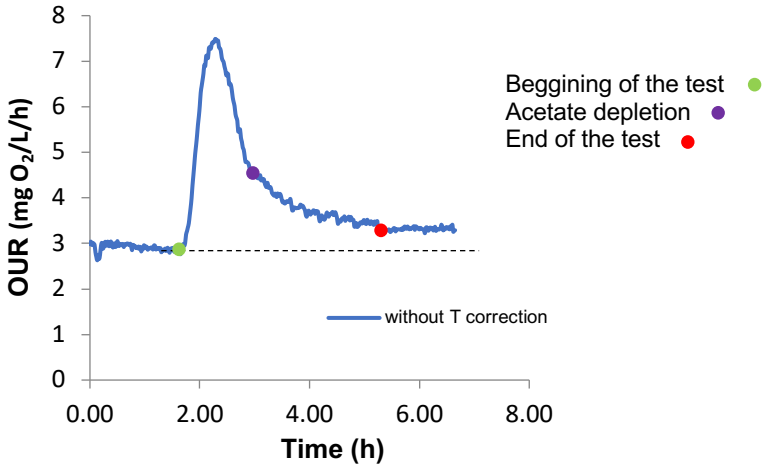

Figure 20: Identification of respirogram key points

The integral between the OUR curve and the line drawn between the two mentioned points is used to calculate Y_H (Figure 21). What follows a situation of storage is the consumption of such storage products, which is translated in the storage yield, Y_{HSTO} (mg_{COD}/mg_{COD}), calculated with the integral defined between the storage line and the endogenous line.

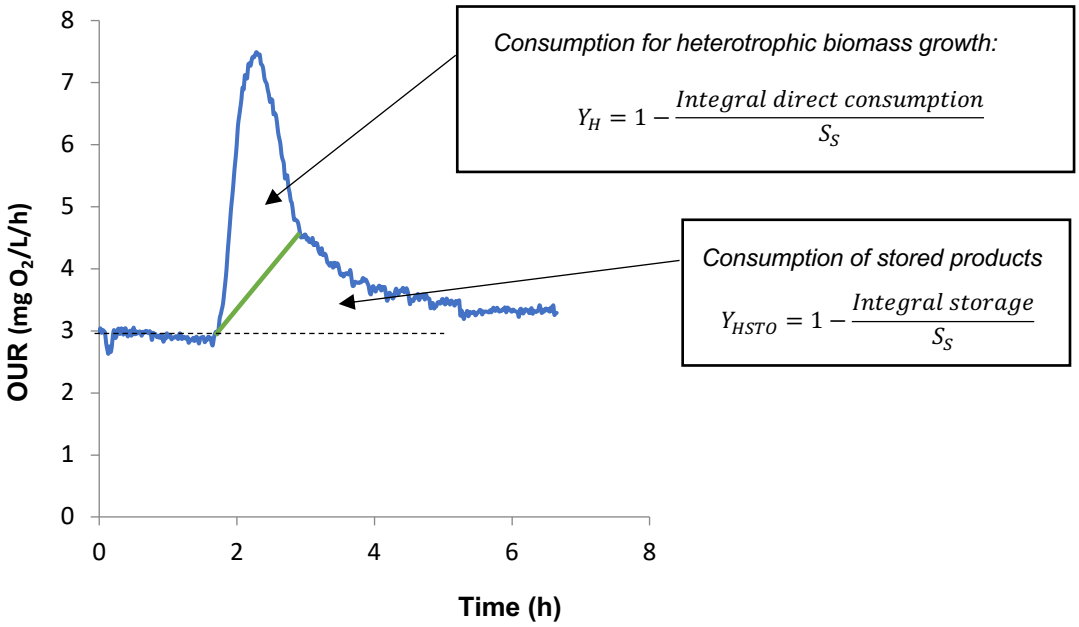

Figure 21: Visual identification of heterotrophic growth yield and storage yield and corresponding calculations

Temperature corrections were also performed to each test, with the simplified Arrhenius equation described in Eq. 28 in sub-section 2.5.3.

From the respirograms obtained in the present work, their respective growth yields Y_H and storage yields Y_{HSTO} were calculated as explained above, and the profiles were classified as I, II and III (Pisoeiro et al. 2017):

- Type I profiles are characterized by an immediate peak in the OUR after S_S addition, followed by the two different slopes corresponding to external substrate consumption and the slower consumption of stored products.
- Type II profiles present a less steep increase of OUR upon S_S addition, compared to the two other types of profiles, resulting in a smaller initial slope.
- Type III profiles are identifiable by a plateau that occurs after SS addition, which is maintained until all of the acetate is consumed.

4.2 Sets of respirometry tests executed

For 6 months, from March to August, 18 successful respirometry tests with sodium acetate trihydrate solution addition were obtained. Of these, 8 were performed with samples from beds with a feeding concentration of 1600 mg/L whilst 10 with beds of 800 mg/L. All resultant OUR profiles are presented below (figure 22 to figure 39), accompanied by the main considerations for each (volume of acetate added in mL, the type of profile, Y_H, and Y_{HSTO}). From Figure 22 to Figure 39, the legend below is applied throughout to distinguish the OUR without (blue) and with (orange) temperature correction.

Legend:

without T correction

with T correction

endogenous level

4.2.1 Respirometry with beds fed with 1600 mg/L concentration in COD

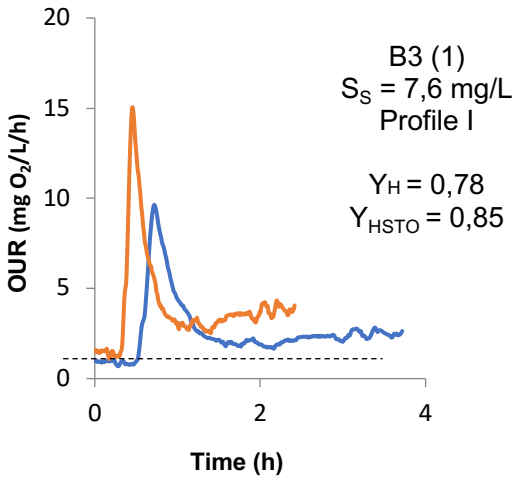

Figure 22: Respirogram B3 (1) from test on 22-03-2018

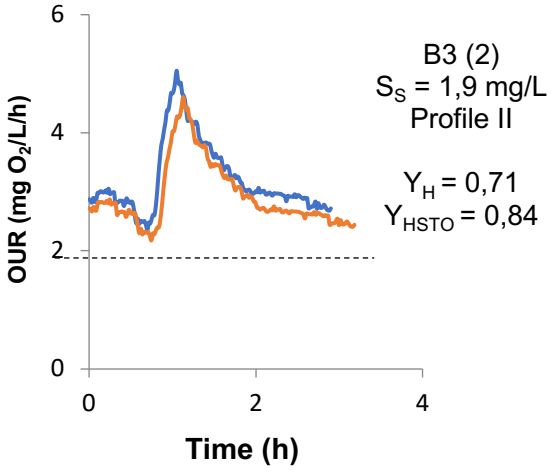

Figure 23: Respirogram B3 (2) from test on 23-04-2018

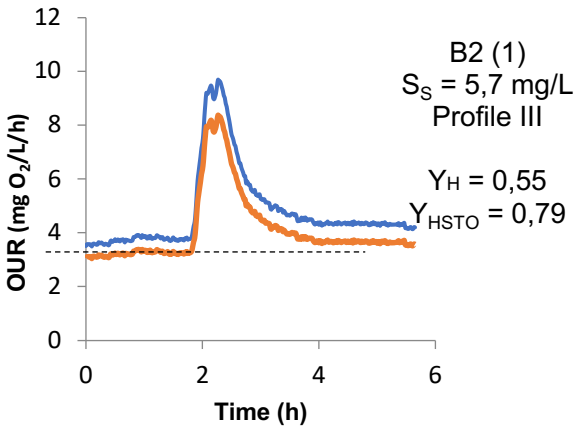

Figure 24: Respirogram B2 (1) from test on 25-05-2018

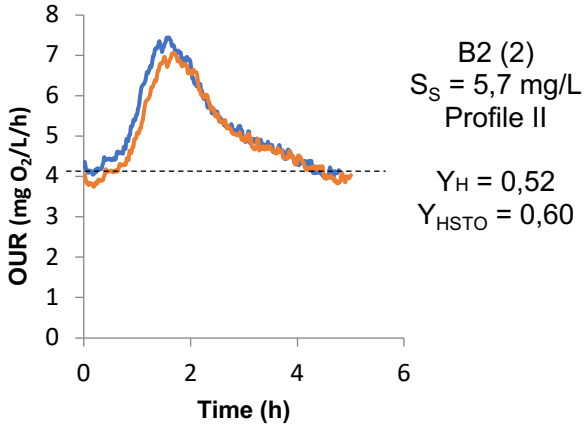

Figure 25: Respirogram B2 (2) from test on 14-06-2018

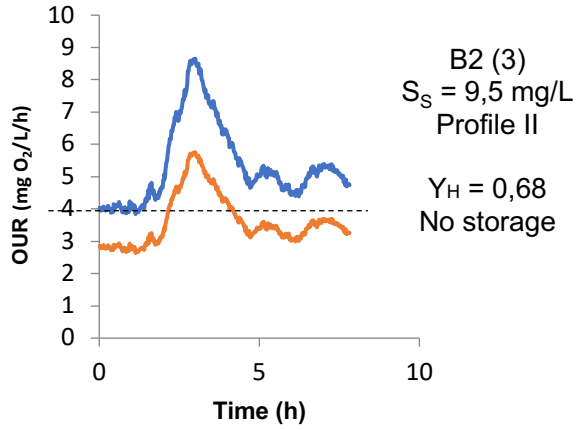

Figure 26: Respirogram B2 (3) from test on 19-06-2018

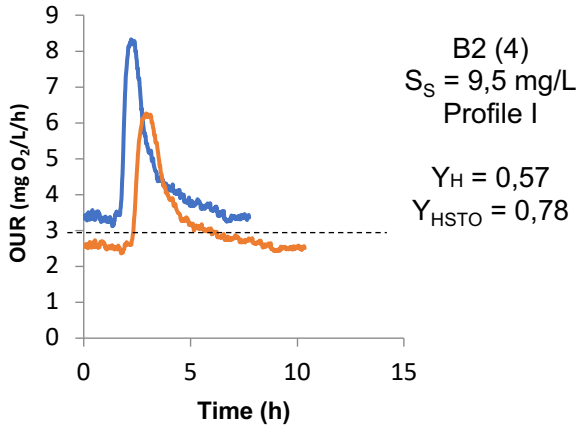

Figure 27: Respirogram B2 (4) from test on 26-06-2018

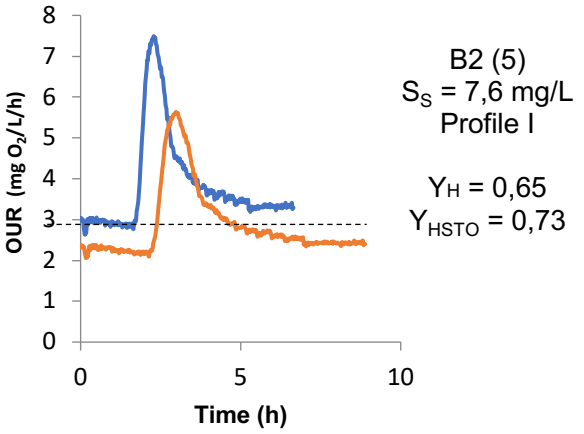

Figure 28: Respirogram B2 (5) from test on 27-06-2018

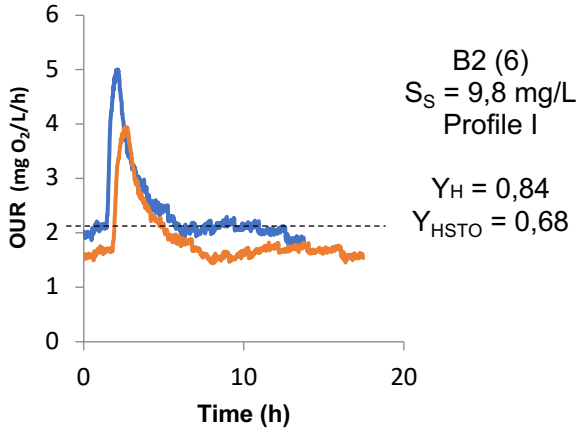

Figure 29: Respirogram B2 (6) from test on 02-07-2018

4.2.2 Respirometry with beds fed with 800 mg/L concentration in COD

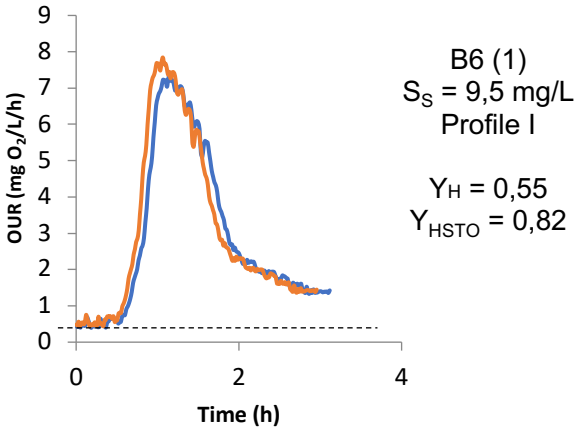

Figure 30: Respirogram B6 (1) from 1st test 15-05-2018

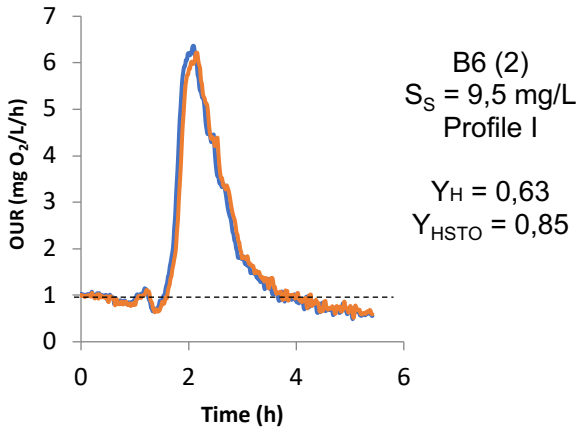

Figure 31: Respirogram B6 (2) from 2nd test 15-05-2018

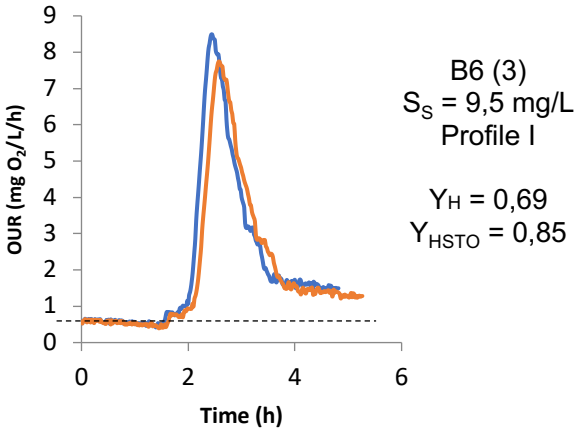

Figure 32: Respirogram B6 (3) from 1st test 16-05-2018

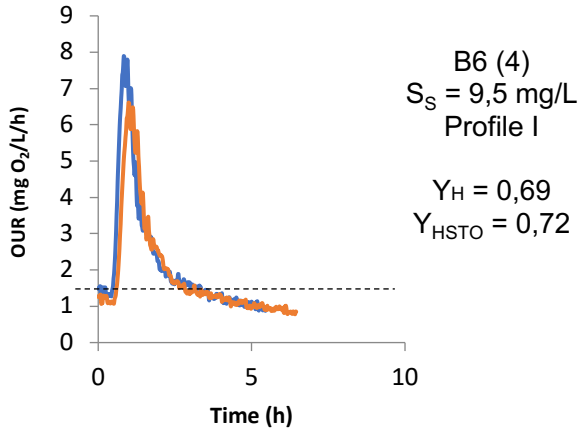

Figure 33: Respirogram B6 (4) from 2nd test 16-05-2018

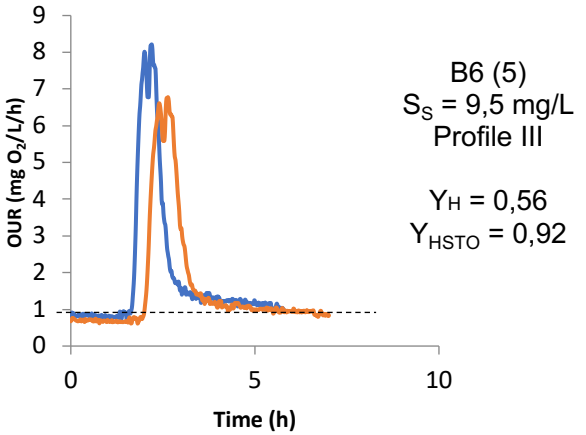

Figure 34: Respirogram B6 (5) from test on 17-05-2018

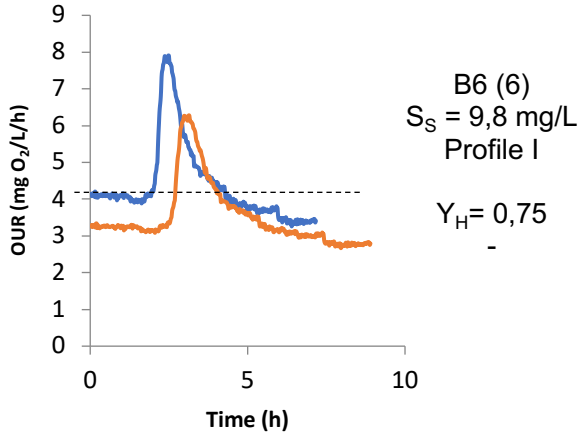

Figure 35: Respirogram B6 (6) from test on 04-07-2018

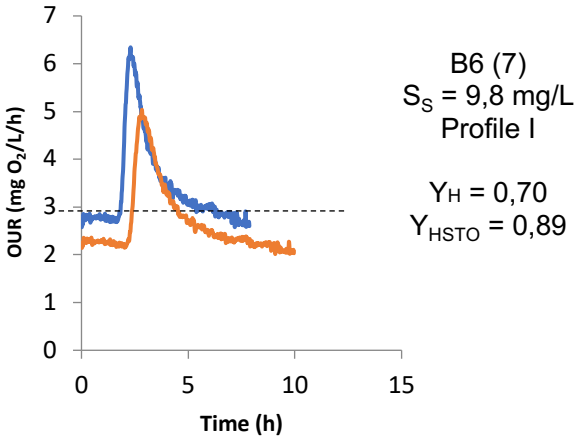

Figure 36: Respirogram B6 (7) from test on 05-07-2018

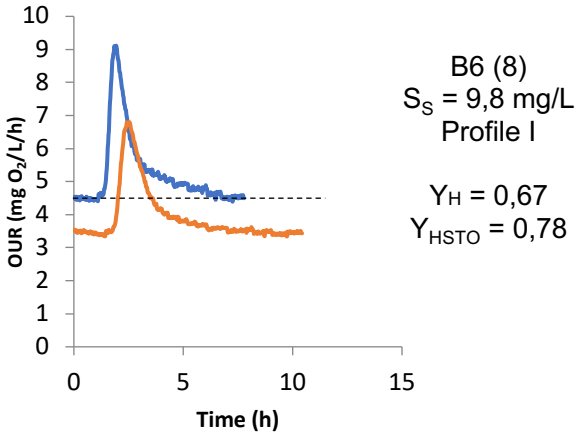

Figure 37: Respirogram B6 (8) from test on 11-07-2018

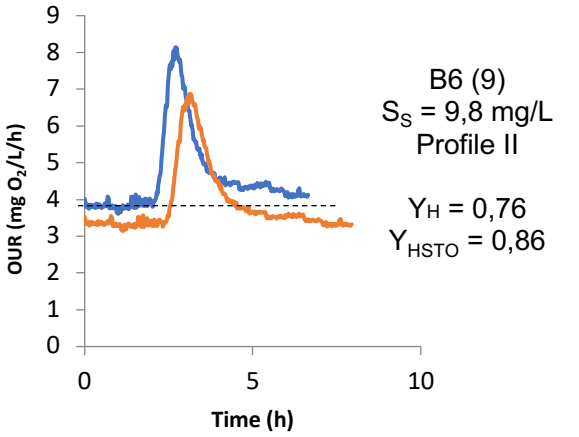

Figure 38: Respirogram B6(9) from 1st test 12-07-2018

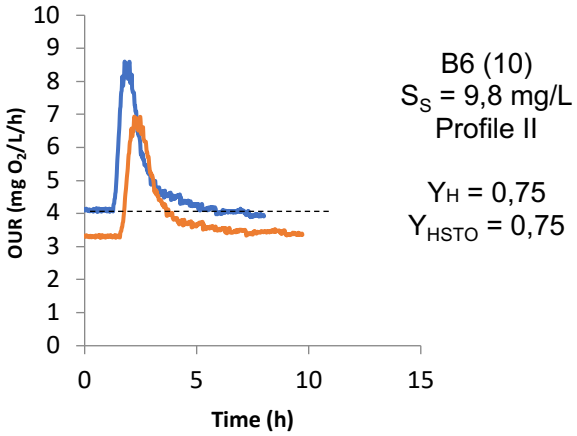

Figure 39: Respirogram B6(10) from 2nd test 12-07-2018

4.2.3 Measured characteristics of the tested beds

As indicated in section 3.3.3, the third and final phase of the respirometric tests is concluded with the assessment of the total fixed and volatile solids of the sampled beds. Table 30 indicates the obtained values for B2 (1600 mg/L) and B6 (800 mg/L), analyzed for TS(g)/gravel(g), FS(g)/gravel(g) and VS(g)/gravel(g). Furthermore, COD readings were performed to the synthetic sewage which fed such beds, as well as to their effluents, allowing for the calculation of the removal efficiency (Table 31).

For the assessment of solids of B_{1600} and B_{800}, several samples were tested from two different extraction sites within the bed, and their average was calculated.

Table 30: Total, fixed and volatile solids ratios to gravel of B_{1600} and B_{800}

	B_{1600}	**B_{800}**
TS/gravel	0,0087	0,0030
FS/gravel	0,0061	0,0011
VS/gravel	0,0026	0,0019

Given that volatile solids are an indicator of the active biomass present in a system, from these measurements one can point out that there is a higher amount of active heterotrophs in B_{1600}. This observation is consistent with the fact that these beds were fed with double the concentration of that for B_{800}.

Regarding the removal efficiency (Table 31), both beds presented very close values of around 95%.

Table 31: Influent and effluent CODs and removal efficiency of beds 2 (B_{1600}) and 6 (B_{800})

	Influent COD (mg/L)	Effluent COD (mg/L)	Removal efficiency (%)
B_{1600}	1578,4	83,9	94,7
B_{800}	714,2	35,0	95,1

Food to microorganism ratio

In order to have a better understanding of the relation between the amount of acetate that was fed and the amount of biomass in each bed, the F:M ratios were calculated for beds 2 (B_{1600}) and 6 (B_{800}).

250 mL of gravel in a graduated cylinder weighted 327 g. This meant that the volume of 1400 mL of gravel in the reactor corresponds to 1831,2 g of gravel.

In order to obtain an average ratio of VS to gravel for each bed, values for their W_{total} and $W_{volatile}$ were used for the relation in Eq. 39, as summarized in Table 32. Given that the weight of each dish in which the sample was weighted was of 2 g, this value is subtracted to that of W_{zero} in order to obtain W_{gravel}.

$$VS\ (g)/gravel\ (g) = \frac{W_{total} - W_{volatile}}{W_{gravel}} = \frac{W_{total} - W_{volaile}}{W_{zero} - 2} \quad (39)$$

Table 32: Volatile solids (g) to gravel (g) ratio for B_{1600} and B_{800} calculated from W_{total} and W_{zero}

	W_{total}	$W_{volatile}$	W_{zero}	VS (g)/gravel (g)	Average VS (g)/gravel (g)
B_{800}	66,767	66,655	66,619	0,0017	0,0019
	61,568	61,442	61,345	0,0021	
	59,579	59,485	59,394	0,0016	
	70,414	70,271	70,174	0,0021	
	64,595	64,480	64,419	0,0018	
	66,455	66,339	66,301	0,0018	
B_{1600}	76,941	76,738	76,216	0,0027	0,0026
	86,353	86,143	85,710	0,0025	

From the average VS/gravel ratios obtained the amount of microorganisms (M) was calculated with Eq. 40 and the amount of food (F) was obtained by multiplying the COD of the acetate by its volume. As in Table 33 summarizes the mentioned values and the F:M ratios obtained for each acetate addition in each bed.

$$M(mg) = VS\ (g)/gravel\ (g) \times 1831{,}2\ (g) \tag{40}$$

Table 33: F:M ratios obtained for different acetate additions

	M (mg)	CQO (mg/L)	Vol. acetate (L)	F (mg)	F:M
B_{1600}	4,801	933,4	0,001	0,933	0,19
			0,003	2,800	0,58
			0,004	3,734	0,78
			0,005	4,667	0,97
		961,4	0,005	4,807	1,00
B_{800}	3,431	933,4	0,005	4,667	1,36
		961,4		4,807	1,40

It is noticeable how for B_{1600} the F:M ratios are lower, which is consistent with the fact that these have a higher amount of microorganisms, as observed by their higher VS/gravel ratios. Given that there are less microorganisms in B_{800}, the F:M ratios are higher, given that there is more food available for the amount of microorganisms.

4.3 Main results from respirometry tests to B_{1600} and B_{800}

The obtained yield values from the tests performed were compiled in Table 36, where the beds were separated according to their concentration. For each test, the concentration of S_S in mg/L and the F:M ratio is also indicated. The type of profile is classified according to Pisoeiro et al. (2017) and each test is identified by the number of the bed (B2, B3 or B6) and the number of the test ((1), (2), …) with the corresponding date.

The set of tests with B_{1600} resulted in four profiles type I, three profiles type II and one type III. A similar distribution of types of profiles was found for the tests to B_{800}, where seven type I, two type II and one type III profiles were obtained. From Table 31 it is also noticeable how the concentration of S_S and the F:M ratio seemingly do not influence the type profile and neither do they seem to influence the yield values.

The pairs B6 (1) and (2), B6 (3) and (4), and B6 (9) and (10) identified with a dashed line, correspond to two tests executed consecutively, under the same conditions and with the same amount of S_S. For each pair, the values obtained for Y_H were fairly consistent between tests, while that of Y_{HSTO} showed a bigger variability. Figure 40 represents the plotting of consecutive B6 (3) and (4) as an example.

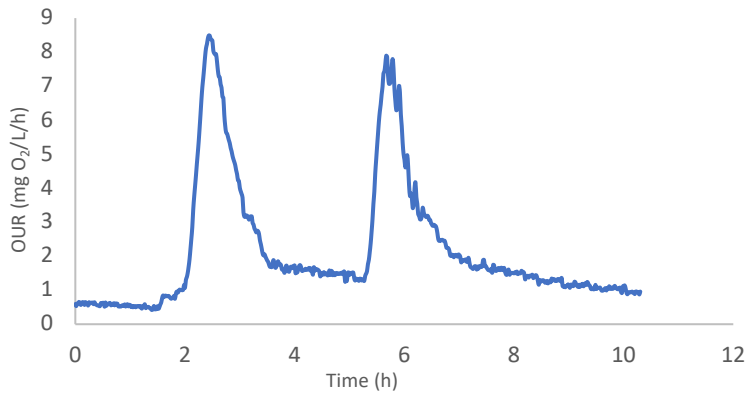

Figure 40: Respirogram of the two consecutive tests, B6 (3) and (4)

The mentioned consecutive tests resulted in the same type of profile, revealing a similar behaviour by the biomass, even if resulting in slightly different yield values.

Table 34: Y_H and Y_{HSTO} values and respective profile types obtained from respirometric tests performed to beds with concentrations of 1600 and 800 mg/L

	Bed designation	Date of the test	S_S (mg/L)	F:M ratio	Type of profile	Y_H (mg_{COD}/mg_{COD})	Y_{HSTO} (mg_{COD}/mg_{COD})	Average Y_H	Average Y_{HSTO}
$B_{1600\ mg/L}$	B3 (1)	22-03-2018	7,6	0,78	I	0,78	0,85	0,66	0,75
	B3 (2)	23-04-2018	1,9	0,19	II	0,71	0,84		
	B2 (1)	25-05-2018	5,7	0,58	III	0,55	0,79		
	B2 (2)	14-06-2018	5,7	0,58	II	0,52	0,60		
	B2 (3)	19-06-2018	9,5	0,97	II	0,68	-		
	B2 (4)	26-06-2018	9,5	0,97	I	0,57	0,78		
	B2 (5)	27-06-2018	7,6	0,78	I	0,65	0,73		
	B2 (6)	02-07-2018	9,8	1,00	I	0,84	0,68		
$B_{800\ mg/L}$	B6 (1)	15-05-2018	9,5	1,36	I	0,55	0,82	0,67	0,83
	B6 (2)	15-05-2018	9,5	1,36	I	0,63	0,85		
	B6 (3)	16-05-2018	9,5	1,36	I	0,69	0,85		
	B6 (4)	16-05-2018	9,5	1,36	I	0,69	0,72		
	B6 (5)	17-05-2018	9,5	1,36	III	0,56	0,92		
	B6 (6)	04-07-2018	9,8	1,40	I	0,75			
	B6 (7)	05-07-2018	9,8	1,40	I	0,70	0,89		
	B6 (8)	11-07-2018	9,8	1,40	I	0,67	0,78		
	B6 (9)	12-07-2018	9,8	1,40	II	0,76	0,86		
	B6 (10)	12-07-2018	9,8	1,40	II	0,75	0,75		

In general terms, comparing the respirometry tests performed to the two types of beds, the results point towards a consistency regarding average values of Y_H for the two types of beds (0,66 for B_{1600} and 0,67 for B_{800}), which indicates that the feeding concentration of the bed does not impact the capacity of the heterotrophs in consuming the substrate for the initial growth phase. When comparing the average values for Y_{HSTO}, these were deemed higher in the case of the beds with a lower concentration, but still similar amongst the two types of beds (0,75 for B_{1600} and 0,83 for B_{800}).

The average values for Y_H and Y_{HSTO} calculated for the 17 tests (excluding test B2 (3) which did not present storage) were respectively of 0,67 (which is close to that indicated by the CWM1 of 0,63) and 0,79.

Even though test B2 (3) did not present storage, its Y_H (in this case, there was only direct S_S consumption for heterotroph growth) still resulted in a value within the average of the remaining tests.

It is also noteworthy how different F:M ratios between B_{1600} and B_{800} resulted in similar yield average values. For example, an F:M ratio of 0,19 resulted in a Y_H of 0,71 and a Y_{HSTO} of 0,84 (test B3 (2)), while with an F:M ratio of 1,40, a Y_H of 0,70 and a Y_{HSTO} of 0,89 were obtained (test B6 (7)). Further information regarding the effect of F:M ratios is presented in subsection 4.3.2.

4.3.1 Classification of respirograms according to type of profile

With the purpose of following the classification and interpretation of the types of profiles by Pisoeiro et al. (2017), Table 35 gathers the value ranges and average values per type of obtained profile in this study.

Table 35: Y_H and Y_{HSTO} value ranges and average values according to each type of profile

Type of profile	no. of tests	Y_H (mg_{COD}/mg_{COD})		Y_{HSTO} (mg_{COD}/mg_{COD})	
		range	average	range	average
I	11	0,55-0,84	0,68	0,68-0,89	0,80
II	5	0,52-0,76	0,68	0,52-0,76	0,76
III	2	0,55-0,56	0,55	0,79-0,92	0,86

The average Y_H values for type I, II and III obtained by Pisoeiro et al. (2017) were of 0,67, 0,41 and 0,48, respectively. Comparing to those obtained in this study, the values for type I profile (0,68) were very similar, and for type III were also close (0,55). The biggest difference obtained was regarding average Y_H for type II (0,68).

Overall, the average growth and storage yield values obtained for the three types of profiles were very similar to the ones by Pisoeiro et al. (2017), with the exception of average Y_H for type II profiles. The same can be said about the value ranges, which were also close to those by Pisoeiro et al. (2017).

As far as the average values for Y_{HSTO}, the ones obtained by Pisoeiro et al. (2017) were of 0,83, 0,75 and 0,83, for types I, II and III. Compared to those of this study, they were in general very similar: 0,80, 0,76 and 0,86.

As in Pisoeiro et al. (2017), the values for Y_{HSTO} in this study were also higher than the Y_H values, indicating the similarity between these two methods for parameter assessment.

In general terms, the frequency of profile type occurrence was found to be similar to that obtained by Pisoeiro et al. (2017): type I profiles are the most common, followed by type II and the rarer type III.

Type I profiles represented the majority of the obtained respirograms, indicating that the general trend by the bacteria is to rapidly respond to the addition of substrate with a steep increase in the consumption of oxygen, followed by a relatively rapid decrease, while still allowing for the consumption of stored products.

The less frequent occurrence of type III profiles indicates that the behaviour of simultaneous growth and substrate storage reflected by the OUR plateau after the peak of S_S addition is not the most common situation verified. For this study, it was found that the higher average values of Y_{HSTO} correspond to this type of profile. Given the low frequency of these profiles, it is difficult to make more accurate remarks concerning typical profile III behaviour. However, the kinetic of this type of profile are that of an immediate response to the S_S addition and of a situation where the heterotrophs are at their maximum consumption during the test, given that there is no shift from feast to famine conditions. Because these were not the conditions sustained during the testing period, the low frequency of occurrence of this type of profiles was expected.

It should be mentioned that the visual resemblance and the similarity in average values and value ranges between profiles of type I and II leads to some difficulties in distinguishing them, which might explain the high count of type I profiles.

Out of the 18 OUR profiles obtained, only one did not reveal storage (test B2 (3)). For the test B6 (6), even though storage is identified visually on its respirogram, the value obtained of Y_{HSTO} was higher than 1,0 and for this reason, it is not presented.

More correlatable values and clearer patterns were expected to be observed with the use of this LSF respirometer, given that it would overcome certain difficulties, such as that of the attachment of the suspended biomass to the probes in the case of the LSS respirometer used by Pisoeiro et al. (2017). Also the attempt to replicate the same conditions (flow, S_S amount, temperature and others) for consecutive tests was expected to produce more similar yield values, which was not observed. For this reason, it is also suggested the study of consecutive respirometric tests, in order to attempt at standardizing the behaviour of active biomass, providing greater robustness to the models under development.

4.3.2 F:M ratio analysis

In an attempt to better explain the obtained results, Y_H and Y_{HSTO} were grouped according to the F:M ratio of each test in Table 36, with their average values and value ranges.

Table 36: Y_H and Y_{HSTO} average values and value ranges according to F:M ratio

F:M	Y_H (mg_{COD}/mg_{COD})		Y_{HSTO} (mg_{COD}/mg_{COD})	
	range	average	range	average
0,19	-	0,71	-	0,84
0,58	0,52-0,55	0,53	0,60-0,79	0,70
0,78	0,65-0,78	0,72	0,73-0,85	0,79
0,97	0,57-0,68	0,62	-	0,78
1,00	-	0,84	-	0,68
1,36	0,55-0,69	0,62	0,72-0,92	0,83
1,40	0,67-0,76	0,73	0,75-0,89	0,82

With the results obtained for this work, it does not seem to be possible to identify a relation between the F:M ratios and the yield values obtained. For instance, the average value of Y_H for an F:M of 0,19 resulted in 0,71 mg_{COD}/mg_{COD}, whilst for a substantially higher F:M of 1,40, the average Y_H resulted in a similar value of 0,73 mg_{COD}/mg_{COD}. The same can be observed for the average values of Y_{HSTO} obtained for different F:M ratios: for a ratio os 0,19, this value is of 0,84 mg_{COD}/mg_{COD}, and for a ratio of 1,36, the average Y_{HSTO} is of 0,83.

5. Conclusions and future works suggestions

A lab-scale HSSF TW replicated as beds (B) fed with different synthetic sewage concentrations (1600 mgO_2/L and 800 mgO_2/L) was successfully sampled and tested with a fixed biomass respirometer – LSF setup – for the assessment of the stoichiometric parameters of heterotrophic growth yield, Y_H and yield on stored substrate, Y_{HSTO}, both in mg_{COD}/mg_{COD}.

Respirometric tests with addition of readily biodegradable substrate in the form of a sodium acetate trihydrate solution resulted in the average Y_H value of 0,66 and 0,67 for B_{1600} and B_{800}, while the average values of Y_{HSTO} were of 0,75 for B_{1600} and of 0,83 for B_{800}. There were no significant differences in the yield values for different F:M ratios.

The average Y_H value of the 18 tests, 0,67, is consistent with that of 0,63, proposed in the general description of the CWM1 (Langergraber et al., 2009).

The classification of the OUR profiles according to the proposed classification by Pisoeiro et al. (2017) of types I, II and III was successfully applied, presenting similarity in the results and indicating thus semblance between the calculation method used in this work and that of the mentioned authors. Particularly, it was found that the majority of the profiles is of type I, where the biomass responds with a peak in the OUR upon Ss addition, correspondent to the initial growth yield, with a subsequent observable behaviour of consumption of stored products. The rare occurrence of type III profiles motivates further studies to supply with more data to the proposed classification.

The use of the LSF respirometer, which proved to be easily assembled with common laboratory materials, has shown promising results when it comes to studying an operating TW, with *ex-situ* analysis made possible by sampling the mentioned wastewater treatment system.

Nonetheless, the variability of the obtained results and the difficulty in correlating them to the F:M ratios or the type of profile obtained still encourages the necessity of respirometric techniques paired with stronger confirmation procedures, such as pH control and more focused food-to-microorganism ratio considerations.

Storage evidence was very strong with the performed tests, where out of 18, only 1 did not present such behaviour. This observation supports the need for further work to be conducted regarding the storage mechanisms that have been explored in the last two decades with the development of models for activated sludge and, more recently, constructed wetlands.

Bibliographic references

Ahansazan, Batool, Hossein Afrashteh, Narges Ahansazan, and Zahra Ahansazan. 2014. “Activated Sludge Process Overview.” *International Journal of Environmental Science and Development* 5 (1): 81–85. https://doi.org/10.7763/IJESD.2014.V5.455.

Alam, Tasnim. 2015. “Estimation of Chemical Oxygen Demand in WasteWater Using UV-VIS Spectroscopy,” 23–25.

Andreottola, G., E. Oliveira, P. Foladori, R. Peterlini, and G. Ziglio. 2007. “Respirometric Techniques for Assessment of Biological Kinetics in Constructed Wetland.” *Water Science and Technology* 56 (3): 255–61. https://doi.org/10.2166/wst.2007.512.

Bilotta, G. S., and R. E. Brazier. 2008. “Understanding the Influence of Suspended Solids on Water Quality and Aquatic Biota.” *Water Research* 42 (12): 2849–61. https://doi.org/10.1016/j.watres.2008.03.018.

Bioscience, Inc. 2016. “Nitrification (Ammonia Oxidation) In Wastewater Treatment Plants.” https://www.bioscienceinc.com/wp-content/uploads/2016/03/Nitrification-Ammonia-Oxidation-in-Wastewater-Treatment-Plants-1.pdf.

Bonner, Ricky, Lara Aylward, Uwe Kappelmeyer, and Craig Sheridan. 2017. “A Comparison of Three Different Residence Time Distribution Modelling Methodologies for Horizontal Subsurface Flow Constructed Wetlands.” *Ecological Engineering* 99: 99–113. https://doi.org/10.1016/j.ecoleng.2016.11.024.

Dotro, Gabriela, Günter Langergraber, Jaume Puigagut, and Otto Stein. 2018. *Biological Wastewater Treatment Series TREATMENT Wetland*. Vol. 7.

Dr. Roshan R. Shrestha. 2008. *Constructed Wetlands Manual*. www.unhabitat.org.

Environmental Protection Agency, EPA. 2001. “METHOD 1683: Total, Fixed, and Volatile Solids in Water, Solids, and Biosolids.” Vol. EPA-821-R-.

Gernaey, Krist V, Mark C M Van Loosdrecht, Mogens Henze, and Morten Lind. 2004. “Activated Sludge Wastewater Treatment Plant Modelling and Simulation : State of the Art” 19: 763–83. https://doi.org/10.1016/j.envsoft.2003.03.005.

Golconda, Abu Zafar. 2016. “Characteristics of Sewage and Treatment Required,” no. January.

Hagman, Marinette, Jes La, and Cour Jansen. 2007. “Oxygen Uptake Rate Measurements for Application at Wastewater Treatment Plants.” *Vatten* 63: 131–38.

Henze, M., W. Gujer, T. Mino, and M. van Loosedrecht. 2000. *Activated Sludge Models ASM1, ASM2, ASM2d and ASM3*. *IWA Publishing*. https://doi.org/10.2166/9781780402369.

Hoque, Muhammad Azizul. 2010. “Development and Calibration of Biokinetic Models for Organic Carbon and Nitrogen Biodegradation in an Aerobic Activated Sludge System.” University of Southern Queensland.

IAWQ Task Group on Respirometry., H., H. Spanjers, G. International Association on Water Quality., and P.L. Dold. 1998. “Respirometry in Control of the Activated Sludge Process : Principles,” no. January: 48.

Indian Institute of Tecnhology. n.d. “Classification Of Water Pollutants And Effects On Environment.” In *NPTEL IIT Kharagpur Web Courses*, 1–7. http://nptel.ac.in/courses/105105048/M10L12.pdf.

Jeppsson, Ulf. 1996. “A General Description of the Activated Sludge” 1 (1996): 1–16.

Langergraber, Guenter, Diederik P L Rousseau, Joan García, and Javier Mena. 2009. “CWM1: A General Model to Describe Biokinetic Processes in Subsurface Flow Constructed Wetlands.” *Water Science and Technology* 59 (9): 1687–97. https://doi.org/10.2166/wst.2009.131.

Lee, Chang Gyun, Tim D. Fletcher, and Guangzhi Sun. 2009. “Nitrogen Removal in Constructed Wetland Systems.” *Engineering in Life Sciences* 9 (1): 11–22. https://doi.org/10.1002/elsc.200800049.

Liwarska-bizukojc, E W A. 2011. “DETERMINATION OF KINETIC AND STOICHIOMETRIC PARAMETERS OF ACTIVATED SLUDGE MODELS An” 37 (3).

Loosdrecht, M. C. M. Van, C. M. Lopez-Vazquez, S. C. F. Meijer, C. M. Hooijmans, and D. Brdjanovic. 2015. “Twenty-Five Years of ASM1: Past, Present and Future of Wastewater Treatment Modelling.” *Journal of Hydroinformatics* 17 (5): 697–718. https://doi.org/10.2166/hydro.2015.006.

Mackenzie, L. Davis. 2010. *Water and Wastewater Engineering*. *McGraw Hill*.

Manios, T., E. I. Stentiford, and P. Millner. 2003. “Removal of Total Suspended Solids from Wastewater in Constructed Horizontal Flow Subsurface Wetlands.” *Journal of Environmental Science and Health - Part A Toxic/Hazardous Substances and Environmental Engineering* 38 (6): 1073–85. https://doi.org/10.1081/ESE-120019865.

Mardani, Sh, A Mirbagheri, M M Amin, and M Ghasemian. 2011. “Determination of Biokinetic

Coefficients for Activated Sludge Processes on Municipal Wastewater." *Iranian Journal of Environmental Health Science & Engineering* 8 (1): 25–25. http://www.bioline.org.br/pdf?se11003.
Meng, Panpan, Haiyan Pei, Wenrong Hu, Yuanyuan Shao, and Zheng Li. 2014. "How to Increase Microbial Degradation in Constructed Wetlands: Influencing Factors and Improvement Measures." *Bioresource Technology* 157: 316–26. https://doi.org/10.1016/j.biortech.2014.01.095.
Ministério do Ambiente. 1997. "Decreto-Lei Nº 152/97 de 19 de Junho de 1997." *Diário Da República - 1 Série-A* Nº 139: 2959–67. https://dre.pt/application/file/a/365412.
Montgomery, Tad. n.d. "Constructed Wetlands to Treat Wastewater - Framework and Schematic Overview." WASTEWATER GARDENS INTERNATIONAL INFORMATION SHEET IS20120105.
Norton, Stephen. 2003. "Removal Mechanisms in Constructed Wastewater Wetlands Stephen Norton." *Removal Mechanisms in Constructed Wastewater Wetlands*.
Petersen, B, and K Gernaey. 2003. "Calibration of Activated Sludge Models: A Critical Review of Experimental Designs" 39 (12): 2459–74. https://doi.org/10.1016/j.watres.2005.05.006.
Pisoeiro, J., A. Galvão, H. M. Pinheiro, F. Ferreira, and J. Matos. 2017. "Determining Stoichiometric Parameters of Detached Biomass from a HSSF-CW Using Respirometry." *Ecological Engineering* 98: 388–93. https://doi.org/10.1016/j.ecoleng.2016.07.003.
Renata, Angela, and Cordeiro Ortigara. 2013. "On the Use of Constructed Wetlands in Mountain Regions : Innovative Tools and Configurations."
Scott, Troy M, Joan B Rose, Tracie M Jenkins, R Samuel, Jerzy Lukasik, and Samuel R Farrah. 2002. "Microbial Source Tracking : Current Methodology and Future Directions Microbial Source Tracking : Current Methodology and Future Directions †." *Applied and Environmental Microbiology* 68 (12): 5796–5803. https://doi.org/10.1128/AEM.68.12.5796.
Sin, Gürkan, Albert Guisasola, Dirk J W De Pauw, Juan A. Baeza, Julián Carrera, and Peter A. Vanrolleghem. 2005. "A New Approach for Modelling Simultaneous Storage and Growth Processes for Activated Sludge Systems under Aerobic Conditions." *Biotechnology and Bioengineering* 92 (5): 600–613. https://doi.org/10.1002/bit.20741.
Sousa, E.R. 2001. "Noções Sobre Qualidade Da Água." *Notas de Hidráulica e Dos Recursos Hídricos e Ambientais* IST: 27. https://goo.gl/NHg6ry.
Spanjers, H., P. Vanrolleghem, G. Olsson, and P. Dold. 1996. "Respirometry in Control of the Activated Sludge Process." *Water Science and Technology* 34 (3–4–4 pt 2): 117–26. https://doi.org/10.1016/0273-1223(96)84211-9.
Spanjers, Henri, and Peter Vanrolleghem. 1995. "Respirometry as a Tool for Rapid Characterization of Waste-Water and Activated-Sludge." *Water Science and Technology* 31 (2): 105–14. https://doi.org/10.2166/wst.1995.0082.
Spanjers, Henri, Peter A Vanrolleghem, and George A Ekama. 2016. *3 Respirometry*. Vol. 9781780404.
Sperling, Marcos Von. 2008. *Wastewater Characteristics, Treatment and Disposal*. *Choice Reviews Online*. Vol. 45. https://doi.org/10.5860/CHOICE.45-2633.
Stairs, Darrin B. 1993. "Flow Characteristics of Constructed Wetlands: Tracer Studies of the Hydraulic Regime."
UNEP. 2016. *A Snapshot of the World's Water Quality: Towards a Global Assessment*. https://doi.org/978-92-807-3555-0.
Vanrolleghem, Peter A. 2002. "Principles of Respirometry in Activated Sludge Wastewater Treatment." *Department of Applied Mathematics, Biometrics and Process Control . Belgium* 32 (9): 1–19.
Vymazal, Jan. 2005. "Horizontal Sub-Surface Flow and Hybrid Constructed Wetlands Systems for Wastewater Treatment." *Ecological Engineering* 25 (5): 478–90. https://doi.org/10.1016/j.ecoleng.2005.07.010.
———. 2007. "Removal of Nutrients in Various Types of Constructed Wetlands." *Science of the Total Environment* 380 (1–3): 48–65. https://doi.org/10.1016/j.scitotenv.2006.09.014.
Vymazal, Jan, Hans Brix, Paul F Cooper, Raimund Haberl, Reinhard Perfler, and Johannes Laber. 1998. "Removal Mechanisms and Types of Constructed Wetlands." *Removal Mechanisms and Types of Constructed Wetlands*.
Vymazal, Jan, and Lenka Kröpfelová. 2009. "Removal of Organics in Constructed Wetlands with Horizontal Sub-Surface Flow: A Review of the Field Experience." *Science of the Total Environment* 407 (13): 3911–22. https://doi.org/10.1016/j.scitotenv.2008.08.032.